A branched heterochronic pathway regulates the juvenile-to-adult transition in *Caenorhabditis elegans*

Inauguraldissertation

zur

Erlangung der Würde eines Doktors der Philosophie

vorgelegt der

Philosophisch-Naturwissenschaftlichen Fakultät der Universität Basel

von

Chiara Azzi

2022

Genehmigt von der Philosophisch-Naturwissenschaftlichen Fakultät

auf Antrag von

Prof. Dr. Helge Grosshans

Prof. Dr. Dirk Schübeler

Prof. Dr. Luisa Cochella

Basel, 17.November 2020

Prof. Dr. Martin Spiess
Dekan

Summary

Temporal coordination of disparate events is a hallmark of robust organismal development and dedicated genetically encoded mechanisms enable such temporal control. In *Caenorhabditis elegans*, the so-called heterochronic pathway times the onset of juvenile-to-adult (J/A) transition, a highly regulated developmental event that involves coordinated behavior of epidermal cells. According to current models, a linear chain of events triggers the J/A transition: accumulation of the *let-7* miRNA causes silencing of its direct target LIN-41. This enables the accumulation of the transcription factor LIN-29 and consequently the coordinated execution of J/A transition events. However, several reports challenge this simple model. For this reason, we aim to understand how the heterochronic pathway coordinates the execution of the J/A transition.

In this work, we first revisited the architecture of the heterochronic pathway. We found that two LIN-29 isoforms, LIN-29a and LIN-29b, have distinct functions and regulation. Unique functions are not the result of molecular differences but of distinct spatiotemporal expression patterns of the isoforms, generated by the activity of distinct upstream heterochronic genes. Specifically, we identify LIN-41, an RNA-binding protein, and HBL-1, a transcription factor, to shape *lin-29* expression in an isoform-specific manner. While *lin-29a* is under direct translation control by LIN-41, *lin-29b* is either directly or indirectly repressed by HBL-1. Coordination of the activities of LIN-29a and LIN-29b is achieved through LIN-28, an upstream heterochronic gene that regulates both LIN-41 and HBL-1. Thereby, our data demonstrate that coordinated J/A transition involves a branched pathway to achieve timely control of multiple events.

Secondly, *hbl-1* is an important but poorly described heterochronic gene. Our characterization of the HBL-1-LIN-29b parallel arm of the heterochronic pathway suggests that the transcription factor HBL-1 behaves as a core player of this pathway. We propose that further research on *hbl-1* targets and functions will be crucial for a proper understanding of how the heterochronic pathway establishes temporal patterning.

In conclusion, the findings presented in this work provides insight into the architecture, properties and mechanism of a biological timer that temporally controls events occurring during the transition from a juvenile to an adult animal.

Table of contents

1 Introduction

1.1 The nature of developmental timing

Proper timing underlies development. The growth and the formation of functional tissues, organs and organisms from a single cell relies on spatial and temporal regulation of cell division, differentiation, patterning and morphogenesis. On one side, alterations in the timing, organization and synchrony of developmental events cause differences that distinguish individuals or species, producing an evolutionary change. On the other, abnormalities in timing can lead to defects that compromise survival. Consequently, understanding how temporal regulation is achieved in developing systems is a fundamental question in developmental and evolutionary biology. In particular, experimental genetics studies focus on understanding whether timing is governed by specific molecular mechanisms and whether it requires specialized factors, distinct from the ones involved in spatial regulation. Over the last decades, the heterochronic pathway, a timing mechanism, in *Caenorhabditis elegans*, has been discovered and extensively studied. The conservation of many of the components of this pathway and the increasing knowledge of its mechanism of action reveal general principles of timing in animal development.

1.1.1 Heterochrony and the evolution of developmental timing

The changes in timing or duration of developmental processes relative to other events in an organism compared to its ancestor has been termed heterochrony (Smith, 2002). Variations in the timing of developmental events are important for the evolution of morphological differences observed between species. A classic example of evolutionary heterochrony can be observed in the axolotl. Axolotls reach sexual maturity without undergoing metamorphosis, retaining their fins and gills in the juvenile form of other salamanders. Axolotls remain in aquatic environments in this form, instead of moving onto land as other sexually mature salamander species. These morphological variations are the consequence of genetic changes that cause altered production and activity of thyroid hormones that drive metamorphosis.

Two types of evolutionary heterochrony have been proposed: 'growth heterochrony', which considers change in size and shape, and 'sequence heterochrony', which explains phenotypic differences by changes in the timing of developmental events (Keyte and Smith, 2015; Smith, 2002, 2003). For the purpose of this thesis, I will focus on sequence heterochrony.

6

To study changes in relative timing of developmental events across a broad range of taxa, it has been advantageous to focus on heterochronies in the sequence of developmental processes. Sequence heterochrony is classified into two categories: paedomorphosis and peramorphosis. Paedomorphosis results in a juvenile outcome compared to ancestral development, whereas peramorphosis results in an adult phenotype. Each category of sequence heterochrony can result from the variation of three parameters that are fundamental to control of developmental events: the time of onset of a particular developmental process, the time of offset of that process, and the rate at which it occurs (Keyte and Smith, 2015; Smith, 2002, 2003) (Figure 1.1). Focusing on these parameters enable the study of variations in developmental sequences in events such as cell proliferation, formation of a specific tissue, appearance of distinct morphological elements, or even the expression of specific genes at specific sites. Analyzing changes in sequence permits not only understanding the principles of heterochrony independently of any variations in developmental rate and developmental stages but also discovery of developmental regulatory mechanisms governing such sequences at the genetic, molecular and cellular levels.
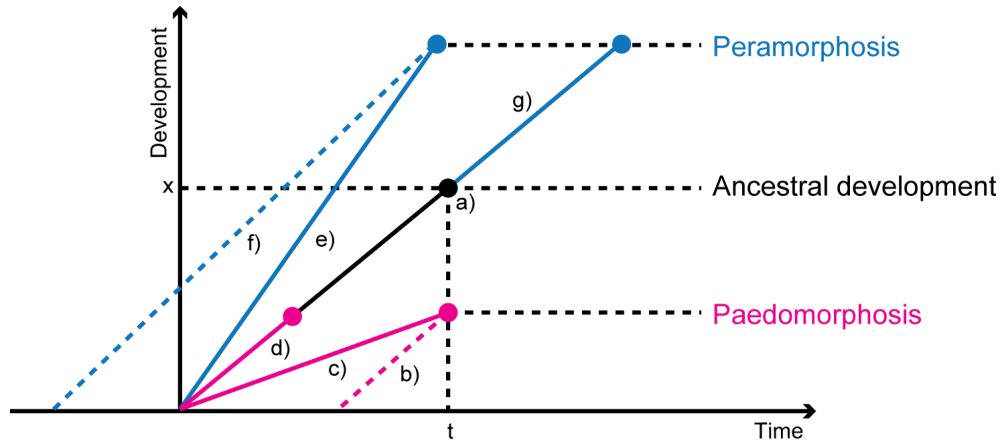
Figure 1.1: Schematic overview of different types of sequence heterochrony

Developmental time is the time needed to reach a certain developmental stage. In normal ancestral development (a) an organism requires time span t to reach development stage x. In Paedomorphosis development is reduced because the onset of development is delayed (b), developmental rate is slowed down (c), the offset of development is happening earlier (d). In Peramorphosis development is extended because the onset of development is earlier (e), developmental rate is accelerated (f), development is reiterated after normal offset (g).

1.1.2 Genetic heterochrony produces significant phenotypic changes

In the last decades, it has been shown that the repertoire of genes among *Metazoa* is highly conserved and the phenotypic differences among organisms are due to changes in the spatial and temporal regulation of these genes. In particular, phenotypic variations are produced by changes in the timing of on- and offset, the rate of expression and the spatial expression pattern. Interestingly, many studies have shown how genetic heterochrony, variations in the relative timing of onset or offset of particular genes, cause major phenotypic change. It appears that subtle change in temporal regulation of different processes can produce significant effects (Smith, 2003). For example, shifts in the expression pattern of the gene *sonic hedgehog* produce morphological variations, specifically digits loss, in different species of the Australian lizard *Hemiergis*. Changes in the timing of gene expression can also cause differences in phenotypic pattern of specific elements, such as different patterns of sensory bristles in three *Drosophila* species due to changes in the rate of gene expression of the *hairy* gene. Moreover, shifts in timing of the appearance of a regulatory factor or receptor, such as hormones during insect development, can cause a switch to an alternative developmental pathway, leading to dramatically different phenotypes in organisms with identical genotypes (reviewed in Smith, 2003). These studies, using genetics to understand how heterochrony produce phenotypic changes, provide a link between microevolutionary processes and macroevolutionary changes.

However, evolutionary heterochrony, since is based on interspecies comparisons, does not allow for drawing conclusions about how developmental timing is regulated in an individual. In order to understand the nature of developmental timing and developmental transitions, studies of heterochrony now specifically address the changes of distinct timing mechanisms, using model organisms.

1.1.3 Diversity of developmental timing mechanisms

In developing organisms, events occur in a particular sequence and it is essential to ensure the correct order of events for a successful outcome. Additionally, it is important to regulate the speed of progression through a developmental sequence. There are diverse regulatory mechanisms that control the order and speed of development, and exemplify the importance of developmental timing to achieve the proper formation of an organism.

In many tissues, cells of different types are produced in a stereotypical sequence from dividing progenitor cells, and the fate of each cell depends on when they are born. The generation of different neuronal and glial subtypes in *Drosophila* ventral nerve cord, the vertebrate retina and cerebral cortex are well-studied examples of such mechanism. In each case, the variations in cell type generation are the result in changes in gene expression program of progenitor cells. In the fruit fly nerve cord, specifically, the activation and repression in turn of four transcription factors specify sequential temporal identity of neurons (Toma et al., 2016).

Timing is the hallmark of the collinearity of Hox genes expression in vertebrate. At the time of gastrulation, the Hox cluster genes are activated sequentially and their expression in time matches their genomic position along the cluster. The temporal order of Hox gene expression depends on different developmental signals. This is an example of how developmental timing mechanism are characterized by properly timed expression of specific genes, even if these genes are not necessary components of the timing mechanism itself (Kmita and Duboule, 2003).

Another type of developmental timing gives rise to vertebrate segmental structure through the process of somite generation. Somites form along the anterior-posterior axis of embryo and are periodically formed from pre-somitic mesoderm in mouse. The rhythmic formation of somites is generated by oscillations in gene expression in the somite precursor cells. Gene expression oscillations slow down as the cells move from their origin, until the oscillations arrest and the cells differentiate based on which oscillating genes are expressed. This molecular oscillator, known as segmentation clock, is driven by components of the Notch signaling pathway and its transcriptional targets, the Hes (Hairy/E(spl)-related) family of transcription factors. The period of oscillations matches the timing of somite formation (Hubaud and Pourquié, 2014).

As the studies of these diverse regulatory mechanisms advance, further principles governing the nature of developmental time will be revealed.

1.1.4 Coordination of multiple developmental processes ensures developmental transitions

Although changing the order and speed of development can have major consequences for one particular tissue, it can also affect other tissues, by changing spatial relationship or signaling interactions, thereby altering the relative order of different events. For this reason,

another fundamental aspect of developmental timing is the coordination between different developmental events to ensure proper tissue organization, patterning, morphogenesis as well as developmental transitions.

The metamorphosis of *Drosophila* larvae is a well-studied example of how coordination of different events has to be regulated to ensure developmental transition. The timing of metamorphosis involves a complex interaction among different tissues and hormones. In particular, the steroid hormone ecdysone, is responsible for triggering molting in larvae and for onset of metamorphosis into the adult fly. Ecdysone binds and activates nuclear hormone receptors, which initiates various gene expression cascades that regulate developmental transitions, establishing the duration of developmental stage and temporal boundaries at molts and pupation. The metamorphosis can be delayed if the imaginal discs, containing the developing organs of the adults, are damaged or their growth is abnormal. In this case, an insulin-like peptide that suppresses ecdysone production is secreted from the imaginal discs. This ensures that after metamorphosis the adults have correct proportions and that wings and legs are of equal size (Thummel, 2001).

Another example of a timing mechanism that involves coordination of multiple events is the regulation of *C. elegans* development. In particular, the heterochronic pathway, a cascade of negative regulators, controls the time and sequence of stage-specific cell-division patterns. The expression of specific heterochronic genes defines each larval stage and the interactions between the components of the pathway promote the transitions between stages (Moss, 2007; Rougvie, 2001; Rougvie and Moss, 2013). How the heterochronic pathway ensures the correct sequence of development and coordinates developmental progression will be explained in detail in the following sections.

1.2 *Caenorhabditis elegans* as a model organism to study temporal regulation of development

Caenorhabditis elegans is a free-living, 1 mm long nematode (roundworm), that lives worldwide in rotten vegetable material and feeds on bacteria and other microorganisms. The worms' small size allows easy cultivation in the laboratory on agar plates containing *Escherichia coli* bacteria as food source, at temperatures ranging from ~15°C to ~25°C. Because of its transparency, it is ideal for microscopy analysis, the visualization of individual cells and tissues is possible using differential interference contrast (DIC) optics and the localization and dynamics of proteins by using fluorescent proteins as tags (as reviewed in Corsi et al., 2015).

C. elegans exists as self-fertilizing hermaphrodites, and as males, which arise spontaneously with a frequency of <0.2%, and allow the exchange of genetic material introducing and combining mutations. In addition, this model organism was the first multicellular organism whose complete genome was sequenced, and forward and reverse genetics have been used to identify numerous genes involved in cell biology and development processes. Finally, a rapid life cycle, of about 3 days at 25 °C from egg to egg-laying adult, as well as large broods, permit efficient expansion of populations and crossing to obtain mutant homozygotes rapidly (as reviewed in Corsi et al., 2015).

The stereotypic development and the known lineage make the worm a great model to study developmental timing. The *C. elegans* life cycle consist of embryogenesis, four larval stages (L1 to L4) and an adult stage. After self-fertilization of the hermaphrodite, or crossing with the male, the embryos develop inside the mother until the 24-cell stage, when they are laid. When the worms hatch, the L1 stage of postembryonic development begins. Every larval stage lasts about 8 hours (at 25°C) and ends with a period of behavioral quiescence (lethargus), during which a new cuticle is made and the old cuticle is shed, a process called molting. In the absence of food or in stressful conditions L2 animals activate an alternative life cycle and molt into an alternative L3 developmental stage, the "dauer" larva (Cassada and Russell, 1975). At the end of the L4 stage the larva turns into an adult. The juvenile-to-adult transition is a highly regulated event (see below), that ensures the end of the larval developmental program and the beginning of the adult post-developmental program (Figure 1.2).

The transparency of *C. elegans* and the invariant number of somatic cells of the worm (959 in an adult hermaphrodite) allowed researchers to track and describe the fate of every cell during development (Kimble and Hirsh, 1979; Sulston and Horvitz, 1977). As a result, the identification of mutations that give rise to developmental defects led to the characterization of molecular pathway involved in regulation of developmental timing. Thus, *C. elegans* is an extremely powerful model organism to study developmental processes and their temporal regulation.

L2

molt 1   molt 2

L3

L1

L2d

molt 3

hatching

dauer

embryo

L4

molt 4

adult hermaphrodite
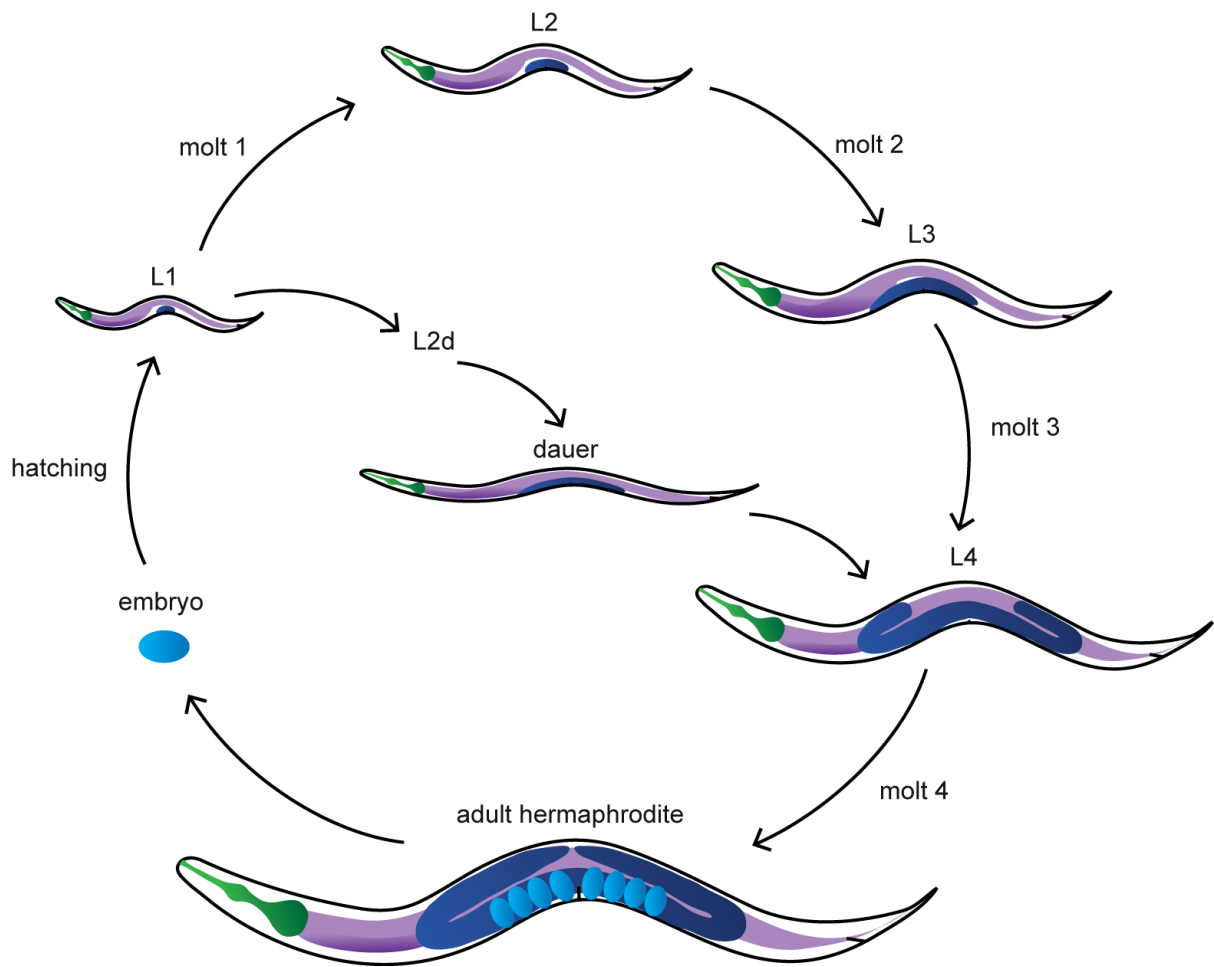
Figure 1.2: *C. elegans* life cycle

After hatching, worms develop through four larval stages (L1-L4), each followed by a molt. After the 4th molt, they develop into a sexually mature adult that lay eggs, from which the next generation of worms will hatch. L1 larvae, under stressful environmental condition, proceed through the alternate dauer pathway (adapted from WormAtlas.com).

1.2.1 The timing of stage specific events in the development of *C. elegans* is controlled by the heterochronic pathway

In *C. elegans*, each cell lineage shows characteristic patterns of cell division and differentiation that occur in a particular sequence and at specific times relative to events of other cell linages (Kimble and Hirsh, 1979; Sulston and Horvitz, 1977). This invariance allowed identification of many genes that when mutated, cause temporal transformations of developmental fates. Ambros and Horvitz first described - as heterochronic mutants - cell lineage mutants that show phenotypes that change timing of a specific developmental event

relative to others happening in the same organism (Ambros and Horvitz, 1984). In these worms, specific cells either prematurely adopt fates of later developmental stages ("precocious" mutants), example of peramorphosis, or repeat fates of earlier developmental stages ("retarded" mutants), example of paedomorphosis. In the last decades, many genes with roles in the heterochronic gene pathway have been identified and their function in regulating the timing of proliferation and differentiation of progenitor cells during larval transitions has been extensively studied.

1.2.2 Juvenile-to-adult transition

The transition from juvenile to adult is a process that involves major physiological changes in an organism. In *C. elegans* the epidermal Juvenile-to-Adult transition (J/A transition) is characterized by multiple events, such as the maturation of sexual organs, the sexually dimorphic differentiation of neurons and the terminal differentiation of seam cells. These developmental events are temporally coordinated by the heterochronic pathway.

This dissertation will focus on the regulation of the epidermal J/A transition, an important event in the development of *C. elegans* epidermal cells. The epidermal J/A transition involves 4 different events happening at different times of development. First, at the L3-to-L4 molt, the seam cells, stem-cell like cells, divide asymmetrically for the last time and cease proliferation. Second, during the mid-L4 stage, seam cells differentiate and fuse into a syncytium. Third, worms produce an adult cuticle, characterized by the presence of adult-specific structures, the alae, and adult-specific collagens. Fourth, animals stop molting after shedding of the L4 larval cuticle (Figure 1.3). These four events have been used as a readout of the J/A transition, and the presence or absence of the events at a defined time of development has been the criteria used to characterize the heterochronic mutants.
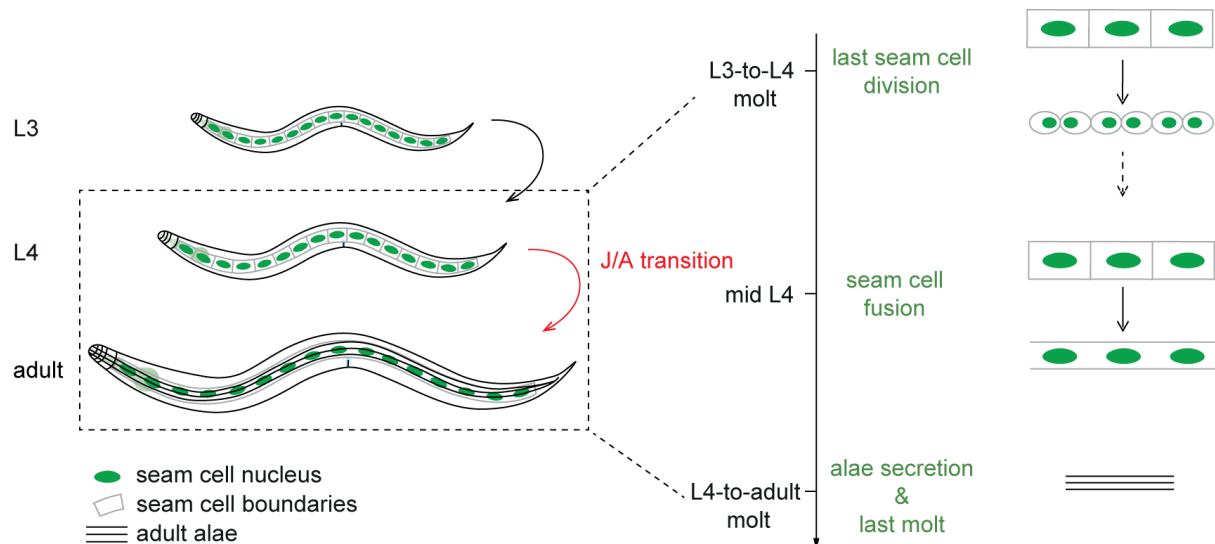
Figure 1.3: The juvenile-to-adult transition in *C. elegans*

The juvenile-to-adult transition comprises four developmental events happening at different times. The final division of seam cells (square-shaped cells with green nuclei) at the L3-to-L4 molt; seam cell fusion into a syncytium during mid-L4 stage; synthesis of an adult cuticle characterized by lateral alae (three horizontal bars) at the L4-to-adult molt; and exit from the molting cycle (Azzi et al., 2020).

1.2.3 Seam cell division and differentiation are timed and coordinated by the heterochronic pathway

The skin of the nematode is composed of a simple epidermal epithelium with an internal basal surface covered by a basal lamina and an apical surface that secretes a cuticle made of collagens (Figure 1.4A). The *C. elegans* post-embryonic epidermis comprises three major cell types, each with different roles in epidermal development: seam cells, postmitotic epidermal cells and ventral epidermal cells.

Although the heterochronic pathway regulates the development of different tissues, much of the research on it has focused on the regulation of proliferation and differentiation of the seam cells. The seam cells are two chains of lateral epidermal cells aligned on the right and left midlines of *C. elegans* body. At hatching, the seam cells are ten on each side of the animal, named from head to tail H0-H2, V1-V6 and T (Figure 1.4B). All seam cells, with the exception of H0 and T, divide in an asymmetric stem cell-like fashion every larval stage, before the molt. These cell divisions generate an anterior daughter cell that fuses with the hyp7 syncytium and

a posterior daughter cell that remains unfused and continues to divide until the last L4 molt (Figure 1.4C-D). In the L2 stage, the posterior daughters of the V cells undergo an additional symmetric division before the asymmetric seam division, increasing the number of seam cells to sixteen per side (Figure 1.4C).

During the transition to the adult state (L4-to-adult molt) the seam cells terminally differentiate, exit the cell cycle and fuse with each other, forming the bilateral seam syncytia (Sulston and Horvitz, 1977). The seam cell syncytia are important for the synthesis of adult specific cuticle, characterized by adult specific collagens, and are responsible for the formation of the lateral alae, ridges that extend along the two sides of the worm and that are formed over the seam cells (Singh and Sulston, 1978). The observation of adult alae is another indicator of seam cell terminal differentiation. Thus, different cellular processes such as cell-cycle exit, cell fusion and production of adult cuticle have to be tightly coordinated during the transition from the proliferative juvenile state to the terminally differentiated adult state in the seam cell lineage.

Regarding the other two cell types that are contained in the hypodermis, the postmitotic epidermal cells derive from the fusion of epidermal precursor cells during embryogenesis and generates the multinucleate syncytia hyp1 through hyp11. The hyp7 syncytium covers much of the larval worm body and increases in size during development, reaching 139 nuclei in adulthood, since in each larval stage additional cells fuse to the hyp7. The twelve ventral epidermal cells P1-P12, during the early L1 stage migrate to the ventral nerve cord, where each P cell divides generating an anterior Pn.a neuroblast and a posterior Pn.p cell. Pn.p cells either fuse to the hyp7 syncytium or remain unfused until the L3 stage when they participate in vulva or mail tail development (reviewed in Chishom and Hsiao, 2012). It is reported that the heterochronic pathway regulates the timing of cell divisions in the P cells and promotes vulva and mail tail formation.
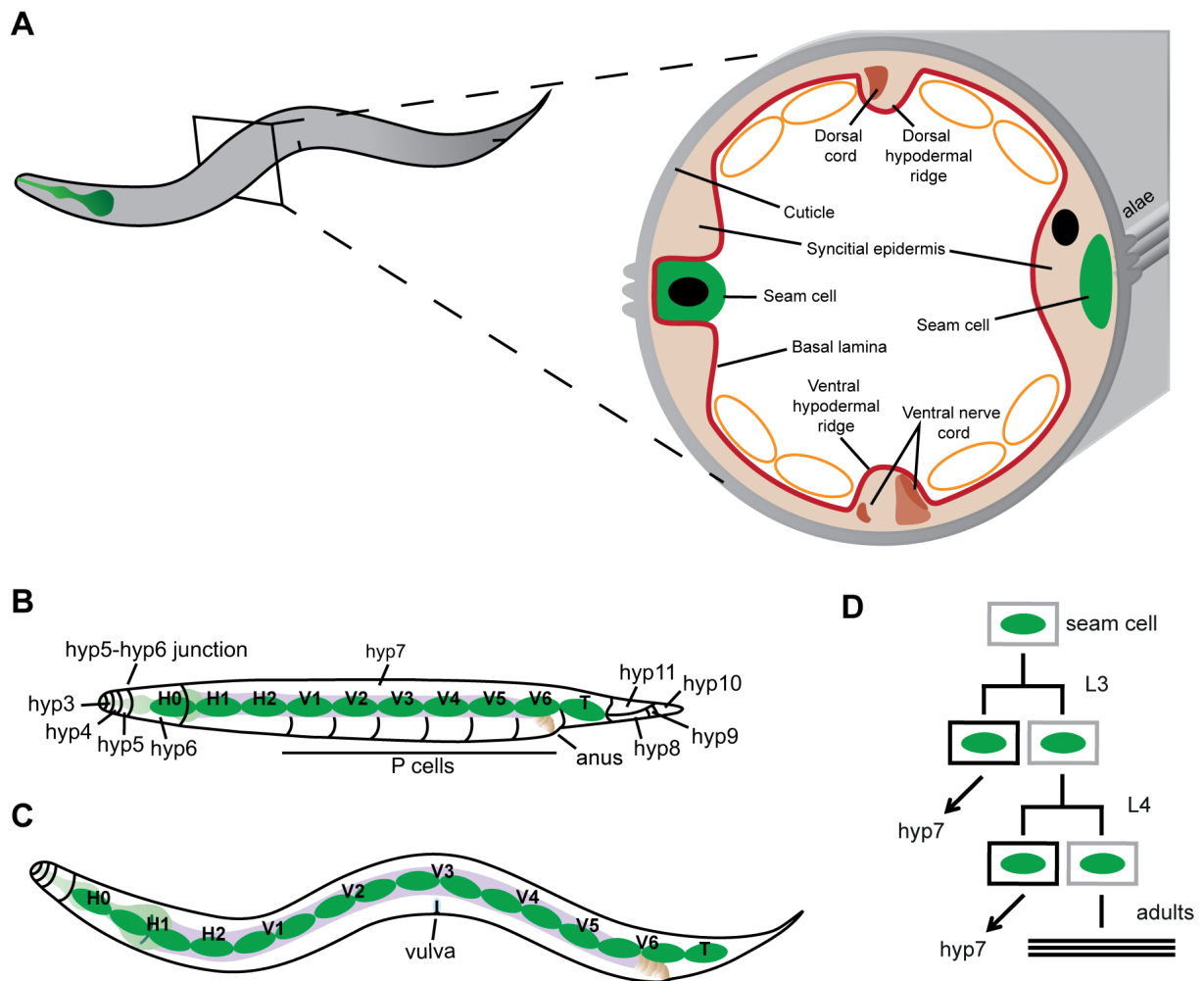
Figure 1.4: The heterochronic pathway regulates epidermal cell fate transition

(A) Cross section of the mid body of an adult hermaphrodite adapted from Wormatlas (https://www.wormatlas.org). The external surface of the worm is covered by the cuticle; the internal face is covered by basal lamina, which contains seam cells and syncytial epidermis.

(B) Schematic view of left lateral seam cells in an L1-stage larva adapted from Wormatlas (https://www.wormatlas.org). In the L1 stage 10 seam cell align on each side of the worm.

(C) Schematic view of left lateral seam cells in adult hermaphrodite. Seam cell number has increased to 16 on each side through seam divisions.

(D) Schematic representation of the asymmetric seam cell division for V1-V4 and V6. At the end of each larval stage, seam cells divide and give rise to another seam cell (gray) and a cell that fuses to the hyp7 syncytium (black). At the L4-to-adult molt, the seam cells terminally differentiate and do not divide again (three horizontal bars).

1.3 The heterochronic genes control developmental transitions in *C. elegans*

Mutations in the heterochronic genes give rise to two different kinds of phenotypes. On the one hand, precocious phenotypes, where the juvenile-to-adult transition events occur earlier in time (for example at the L3 to L4 molt) and stage-specific events are skipped, as observed in *lin-14*, *lin-28*, *lin-41* or *hbl-1* mutants. On the other, retarded phenotypes, where the J/A transition fails to occur or is delayed and stage-specific events are reiterated, such as in the *lin-4*, *let-7*, three *let-7* sisters or *lin-29* mutants. The core heterochronic pathway takes advantage of transcriptional and post-transcriptional mechanisms to control development since it is composed of transcription factors, miRNAs and RNA binding proteins. In the last decades, the knowledge of genetic interactions between the players of the core pathway has grown and models in which each gene contributes to a linear chain of events to trigger the J/A transition have been proposed (Figure 1.5A). These models depict the heterochronic pathway as a cascade of negative regulators. The miRNA *lin-4* accumulates during the L1 stage to inhibit the transcription factor LIN-14 and the RNA binding protein LIN-28. When LIN-28 is downregulated, its negative regulation on the miRNA *let-7* is released and, consequently, *let-7* can accumulate during the L3 stage to inhibit synthesis of the RNA binding protein LIN-41. Since LIN-41 translationally represses *lin-29*, its decreased levels during L4 allow the accumulation of the transcription factor LIN-29. Such accumulation of LIN-29 ensures the coordinated execution of the J/A transition events (Figure 1.5B). However, there are genes of the core pathway, such as *hbl-1*, whose placement in such linear model is still debated. Moreover, the described molecular functions and interactions among the heterochronic genes requires better characterization in order to fully understand the molecular mechanism that regulate cell-fate transitions.

In order to discuss the function and the relationships of the genes of the pathway, I decided to divide the heterochronic pathway in three different phases, as done before (Rougvie and Moss, 2013). Each phase involves specific players of the heterochronic pathway that allow the transition to the next phase. In particular, the three transcription factors LIN-14, HBL-1, LIN-29 control the transitions from earlier to later stages, and are temporally regulated, directly or indirectly, by upstream heterochronic genes encoding microRNAs and RNA binding proteins. I will focus in particular on two of the transcription factors, LIN-29 and HBL-1, because of their relevance for this dissertation. Other heterochronic genes and their role in

regulating developmental timing, such as *daf-12* or *lin-42*, will not be discussed in this thesis, but they are reviewed elsewhere (Rougvie and Moss, 2013).
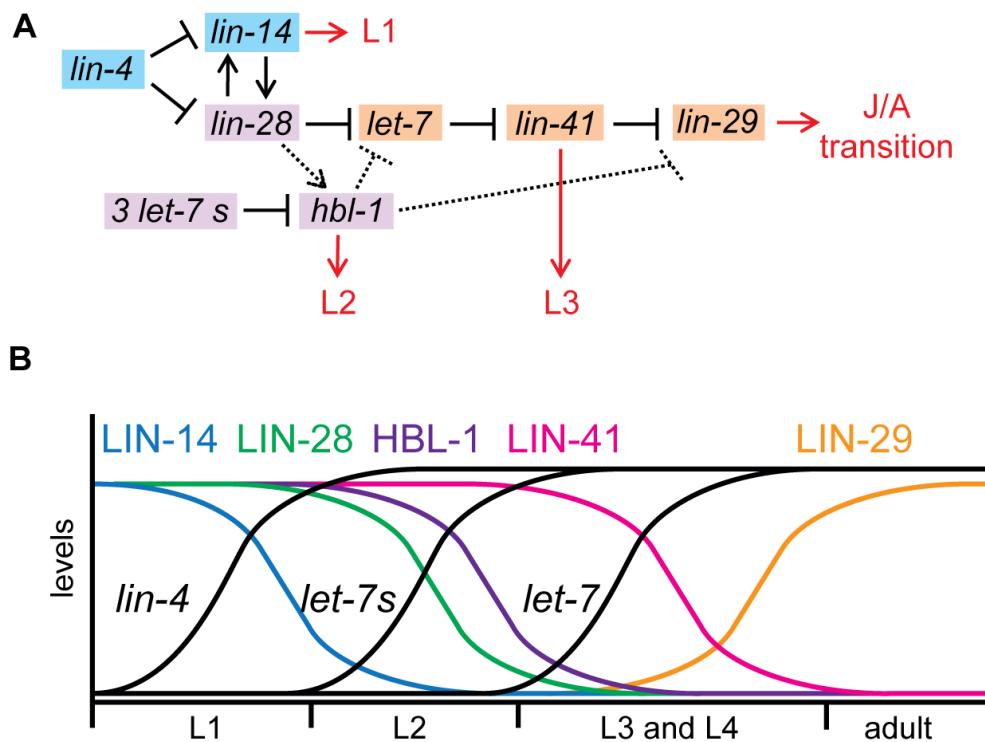
Figure 1.5: Genetic and dynamic models of the heterochronic pathway

(A) Model of the genetic interactions between the core regulators of the heterochronic pathway. Unclear molecular links are indicated with dashed lines. Stage-specific fates are indicated by larval stages and J/A transition. Genes shaded in blue are components of the first phase, genes squared in violet of the second phase, genes squared in orange of the third phase. (B) Representative model of the gene expression profiles of the product of key heterochronic genes. miRNAs, depicted in black, are off at the beginning of development and rise at specific times, downregulation or upregulation of RNA binding proteins and transcription factors is depicted in different colors.

1.3.1 *lin-4* and *lin-14* constitute the first phase promoting the L1-to-L2 transition

lin-4 and *lin-14* are components of the first phase and specify the developmental transition from the L1 to the L2 stage. *lin-4* is the first described microRNA (Lee et al., 1993), which begins to accumulate in mid-L1 stage worms and is constitutively expressed thereafter. *lin-4* is necessary to initiate the progression from L1 to L2 stage, by downregulating LIN-14 and

LIN-28 by binding to the 3'UTR of their mRNAs (Lee et al., 1993; Moss et al., 1997; Wightman et al., 1993). *lin-4* loss-of-function (lf) mutants show a retarded phenotype, in fact they reiterate the L1 division of seam cells, and the terminal differentiation of the epidermis never occurs. This phenotype is due to the failure of the downregulation of its target, the transcription factor LIN-14. Consistently, *lin-14* gain-of-function (gf) mutant animals show the same retarded phenotype of *lin-4(lf)* mutants. LIN-14 protein is normally accumulated in early L1 worms and is downregulated as development proceeds (Ruvkun and Giusto, 1989). A loss-of-function mutation in *lin-14* causes a precocious phenotype, omitting the L1 stage and directly showing the symmetric division characteristic of the L2 stage (Ambros and Horvitz, 1984). Consequently, in *lin-14(lf)* animals, the juvenile-to-adult transition occurs after only three molts (Ambros and Horvitz, 1984). Moreover, *lin-14* function is defined by two separable and sequential activities, which, however, do not appear to correspond to gene isoforms. On the one hand, *lin-14a* specifies the L1 rather the L2 lineage pattern, on the other *lin-14b* acts in the late L1 stage to prevent precocious expression of the L3 pattern in the L2 (Ambros and Horvitz, 1987). But the downregulation of both *lin-14* isoforms by *lin-4* is crucial for the L1- to-L2 developmental transition (Ambros and Horvitz, 1987; Lee et al., 1993; Wightman et al., 1993).

1.3.2 *lin-28* and *hbl-1* govern the second phase of the heterochronic pathway

The transition from L2 to L3 stage, the second phase, has as major regulators the RNA binding protein *lin-28* and the transcription factor *hbl-1*. LIN-28 is known to have an important role in different transitions during larval development and reported to have two separable activities. *lin-28* is the second target of *lin-4* miRNA and its expression is down-regulated by the L3 stage. LIN-28's major and most studied role is the inhibition of the accumulation of the mature *let-7* miRNA in early stages of development. LIN-28 binds the precursor of the *let-7* microRNAs and block its processing by recruiting a poly(U) polymerase that promotes the degradation of the precursor *let-7* RNA (Lehrbach et al., 2009; Viswanathan et al., 2008). It is also known that LIN-28 binds to the primary let-7 transcripts co-transcriptionally, and this interaction blocks its processing to pre-*let-7* by Drosha (Van Wynsberghe et al., 2011). Thus, the accumulation of mature *let-7* is prevented until *lin-28* is targeted by *lin-4* (Moss et al., 1997). However, even if the control of *let-7* accumulation by LIN-28, and the consequent positive regulation of *lin-41*, is a function of this protein that governs the L3-to-L4 transition,

the first of *lin-28*'s activity is the regulation of the L2-to-L3 transition, independently of *let-7* (Vadla et al., 2012). *lin-28* mutants, indeed, show a precocious phenotype, skipping the L2 stage specific pattern of seam cell divisions. This suggest that LIN-28 has an important role in the promotion of the L2 stage specific events. This function could be explained by the positive regulation of *hbl-1* by *lin-28*, but the mechanism that drives such regulation is still unclear (Ilbay and Ambros, 2019; Vadla et al., 2012). In addition, *lin-28* positively regulates LIN-14 expression and *lin-14* is required for wild type accumulation of LIN-28, since in *lin-28(lf)* mutants, *lin-14* is repressed, and in *lin-14(lf)* mutants, *lin-28* is not detected (Arasu and Hospital, 1991; Moss et al., 1997). The positive feedback loop between *lin-28* and *lin-14* and their temporally regulated downregulation indicates that these two players of the heterochronic pathway are fundamental in the control of early larval development. Thus, *lin-28* is a stage specific key regulator of the heterochronic pathway that positively influences three other stage specific players of the pathway, *lin-14*, *hbl-1* and *lin-41*.

The other important effectors of the second phase are *hbl-1* and the *let-7* sister miRNAs. The three miRNAs - miR-48, miR-84 and miR-241 - share the same seed sequence with *let-7* miRNA and for this reason they are considered part of the so called *let-7* family. The seed sequence is a conserved sequence situated at positions 2-8 from the 5'-end of the miRNA and is the main determinant for target identification and silencing (Bartel, 2009). The three sisters accumulate in early L2 larvae and their levels remain high throughout development, their upregulation is needed to initiate the L2-to-L3 transition (Abbott et al., 2005; Reinhart et al., 2000; Vadla et al., 2012). miR-48, miR-84 and miR-241 act redundantly to repress their main target, *hbl-1* (Abbott et al., 2005). *mir-48/241/84* triple mutant animals show a retarded phenotype characterized by reiteration of the L2 symmetrical seam cells division and do not go through the juvenile-to-adult transition (Abbott et al., 2005). Moreover, it has been shown that miR-48/241/84 are not fully redundant with *let-7* since, despite having complementary sites in the 3'UTR of other heterochronic genes such as *lin-41* and *lin-28*, it seems that miR-48/241/84 do not regulate these genes (Brancati and Großhans, 2018). In fact, only *hbl-1* depletion suppresses the *mir-48*; *mir-84*; *mir-241* triple mutant phenotype, not *lin-41*, and only the downregulation of *hbl-1*, not *lin-28*, is *let-7* sisters dependent (Abbott et al., 2005). *hbl-1* is the other key effector of the second phase. The role of this transcription factor in the heterochronic pathway is still unclear. However, it has been shown that HBL-1 downregulation is fundamental to progress from the L2 to the L3 stage (Abbott et al., 2005; Abrahante et al.,

2003; Lin et al., 2003). *hbl-1* as a player of the heterochronic pathway and its role in the regulating developmental transition will be discussed in detail in section 1.3.3.

1.3.3 HBL-1, a regulator of different developmental transitions

The *hbl-1* (*hunchback-like*) gene encodes a zinc finger transcription factor of the Hunchback/Ikaros family. Published work on the function of *hbl-1* in *C. elegans* development relies on hypomorph, reduction-of-function (rf), mutation or HBL-1 depletion by RNAi, because *hbl-1* null mutants die during embryogenesis (Fay et al., 1999). For this reason, the function and the position of *hbl-1* in the heterochronic pathway remains unclear. *hbl-1* mutant animals show precocious phenotypes: seam cells fuse already in the L3 stage, alae formation occurs during the L4 stage and LIN-29 is accumulated precociously. By contrast, these animals go through four molts, indicating that the molting cycle occurs normally (Abrahante et al., 2003; Lin et al., 2003). Nevertheless, it is elusive which larval stage the *hbl-1(rf)* mutant skip, because they show a normal L2-stage specific symmetric seam cells division. Moreover, additional seam cell divisions are observed during the adult stage, suggesting that the terminal differentiation of the seam cells is not complete until the juvenile-to-adult transition (Abrahante et al., 2003; Lin et al., 2003). However, *hbl-1* is reported to have a regulatory function in the transition from L2-to-L3 stage because its downregulation by the miR-48, miR-84 and miR-241 miRNAs is crucial for the transition to happen and for this reason *hbl-1* is considered a key effector of the second phase (Abbott et al., 2005; Rougvie and Moss, 2013). Specifically, in the hyp7, but not in seam cells, *let-7* sisters post-transcriptionally silence *hbl-1*, whereas in the seam cells, but not in the hyp7, HBL-1 is regulated by another heterochronic regulator, LIN-46 (Ilbay and Ambros, 2019; Ilbay et al., 2019). Recently it has been shown that LIN-46 is required for HBL-1 accumulation in the cytoplasm of seam cells, causing consequent reduction of HBL-1 activity in the nucleus, after LIN-46 itself has been released from LIN-28 repression (Ilbay and Ambros, 2019; Ilbay et al., 2019). Moreover, this observation supports the previously shown positive regulation of *hbl-1* by LIN-28 (Vadla et al., 2012).

hbl-1 was also suggested to function in parallel to *lin-41*, by repressing the same target, the transcription factor *lin-29* (Abrahante et al., 2003; Lin et al., 2003). In *hbl-1* and *lin-41* single mutants the seam cells precociously fuse and secrete alae during the fourth larval stage, but the phenotypes are rather weak (Abrahante et al., 2003; Lin et al., 2003; Slack et al., 2000). By contrast, *lin-41;hbl-1* double mutants display a fully penetrant precocious phenotype at the L3-

to-L4 molt, namely secretion of complete alae and exit from the cell cycle of all seam cells, with 50% of the worms showing precocious alae even two stages earlier (Abrahante et al., 2003; Lin et al., 2003). To date, the redundancy between *hbl-1* and *lin-41* remained unsolved since it relies on the study of genetic interactions of hypomorph alleles.

The direct targets through which HBL-1 control temporal cell fates are unknown. Moreover, if *hbl-1* regulates *lin-29* directly or indirectly is not yet understood. In particular, *hbl-1* expression from multicopy transgene arrays seems to be downregulated in seam cells and hyp7 by the L2 stage (Abbott et al., 2005; Abrahante et al., 2003; Lin et al., 2003), yet LIN-29 starts to accumulate in the epidermis at the end of L3 stage and peaks in L4 (Bettinger et al., 1996). This time gap between HBL-1 downregulation and LIN-29 expression could suggest that the available tools are not showing the real *hbl-1* expression pattern, or that some unknown factor could mediate *lin-29* repression.

Interestingly, it was suggested that HBL-1 inhibits the transcription of *let-7* until the L3 stage in the seam cells (Roush and Slack, 2009). From these results it seems possible that HBL-1, together with LIN-28, acts to prevent precocious expression of *let-7*, and consequently of *lin-29a* in the epidermis. Hence, although previous results suggest that *hbl-1* is a critical developmental regulator of also later stages of development, its mechanism of action remains elusive.

1.3.4 The repression of *lin-41* by *let-7* and resulting *lin-29* activation characterize the third phase

The third phase is governed by *let-7*, *lin-41* and *lin-29*. These three factors promote the developmental progression from the L3 stage to adulthood. To date, it is unclear how the heterochronic pathway regulates the L3-to-L4 transition (Rougvie and Moss, 2013), although it was suggested that the switch *let-7*/*lin-41* play a role in regulating the L3 fates (Vadla et al., 2012). The transcription factor LIN-29 is the most downstream gene of the heterochronic pathway and its upregulation at the L4 stage in the epidermis is necessary to promote the seam cell terminal differentiation and the transition from L4-to-adulthood. *lin-29* function will be discussed in detail in section 1.3.5.

The *let-7* miRNA has a prominent role in the maturation of worm sexual organs, controlling the morphogenesis of the vulval-uterine tract in hermaphrodites (Ecsedi et al., 2015) and male tale cell retraction events (Del Rio-Albrechtsen et al., 2006). A *let-7* null

mutation is lethal, the animals die bursting through the vulva at the L4-to-adult transition (Reinhart et al., 2000). On the other side, the accumulation of the *let-7* miRNAs during the L3 stage, and its sustained and high expression during the L4 and adult stage is necessary to initiate the J/A transition (Reinhart et al., 2000). *let-7* targets *lin-41* mRNA, binding its 3'UTR at 2 sites, LCS1 and LCS (*let-7* Complementary Site) (Vella et al., 2004). In *let-7* worms carrying a loss-of-function allele, the seam cell terminal differentiation does not occur, supernumerary seam cells are observed and alae are absent. Moreover, *let7(lf)* mutants undergo a fifth molt and eventually seam cells differentiate and produce alae (Reinhart et al., 2000). This retarded phenotype is due to failed LIN-29 upregulation. *lin-41*, is not the only heterochronic gene targeted by *let-7*; *hbl-1* (Abrahante et al., 2003; Lin et al., 2003) and *daf-12* (Großhans et al., 2005) were shown to be *let-7* targets as well. Interestingly, the depletion of either *lin-41*, *hbl-1* or *daf-12* resulted in suppression of *let-7* retarded phenotypes, restoring events of the J/A transition (Abrahante et al., 2003; Großhans et al., 2005; Lin et al., 2003; Slack et al., 2000). However, it has been recently shown that *let-7* temporally controls morphogenesis of the female and male sexual organs and seam cell fate by silencing *lin-41* as a single target (Aeschimann et al., 2019; Ecsedi et al., 2015).

LIN-41 is a TRIM-NHL protein with an RNA binding protein function involved in the control of seam cell fate specification (Aeschimann et al., 2017). *lin-41* mRNA is downregulated during the L3 and L4 stages when *let-7* targets its 3'UTR and represses its translation. This downregulation has been proposed to be important for both the L3-to-L4 transition and the L4-to-adult transition (Reinhart et al., 2000; Slack et al., 2000; Vadla et al., 2012). LIN-41 has a fundamental role in keeping the larval program on, and it achieves it by mRNA silencing of its targets with two distinct position dependent mechanisms. On the one hand, LIN-41 represses the expression of *lin-29a* by binding its 5'UTR and inhibiting the translational initiation, on the other hand, it represses *mab-10*, LIN-29 co-factor, by binding its 3'UTR and inducing mRNA decay (Aeschimann et al., 2017). Accordingly, *lin-41(lf)* mutant animals show a precocious onset of adult developmental programs, with early seam cell differentiation and alae secretion (Slack et al., 2000). However, this phenotype occurs with incomplete penetrance and only for a subset of seam cells. Interestingly, overexpression of LIN-41 results in a reiteration of the larval stage pattern of seam cells division, as observed for *let-7(lf)* animals, confirming that the activity of LIN-41 must decline to allow LIN-29 to initiate the adult programme (Slack et al., 2000).

1.3.5 LIN-29 is the key effector of the juvenile-to-adult transition

lin-29, encoding an EGR transcription factor, is the most downstream gene identified in the heterochronic pathway and assumed to be the key effector, which executes all four aspects of the J/A transition (Rougvie and Ambros, 1995). Indeed, LIN-29 accumulates during the L4 stage, before the transition to adulthood occurs (Bettinger et al., 1996). *lin-29* null mutant worms progress normally through all larval stages until they reach the end of the L4 stage, when they fail to execute the adult-specific terminal differentiation program and instead repeat the larval program (Ambros and Horvitz, 1984). In all heterochronic mutants where the J/A transition occurs prematurely, the phenotype can be suppressed by additionally mutating *lin-29*, leading to repeated larval cell fates as in *lin-29* single mutants. For this reason, it is likely that the premature J/A transition in the precocious heterochronic mutants is due to an upregulation of the LIN-29 protein in the epidermis (Rougvie and Moss, 2013).

There are two major mRNA isoforms, *lin-29a* and *lin-29b*. The *lin-29a* and *lin-29b* transcripts share the same 3'end but differ in the 5' end since the *lin-29b* transcript begins at the start of exon 5 of the *lin-29a* transcript (Rougvie and Ambros, 1995). LIN-29a and LIN-29b were proposed to redundantly contribute to the same functions since their observed expression pattern was largely similar (Bettinger et al., 1997). LIN-29a and LIN-29b share the same transcription co-factor, MAB-10/NAB. MAB-10 directly binds LIN-29 through a conserved interacting domain and modulates its activity (Harris and Horvitz, 2011). MAB-10, like LIN-29, is required to prevent extra molts and extra seam cell divisions but unlike LIN-29 is not required for adult specific cuticle synthesis or seam cell fusion (Harris and Horvitz, 2011).

Genetic experiments suggested that, in *C. elegans*, *lin-29* is negatively regulated by different heterochronic genes, which act in parallel. On the one hand, the downregulation of the RNA binding protein LIN-41 by the microRNA *let-7* leads to the upregulation of LIN-29, promoting the J/A transition. On the other, the downregulation of the transcription factor HBL-1 by the *let-7 sisters miR-48*, *miR-84* and *miR-241* also promote the upregulation of LIN-29 and consequently the transition. The possibility of a parallel regulation of *lin-29* by upstream heterochronic genes was already suggested by the redundancy between *hbl-1* and *lin-41*. In particular, epistasis experiments showed that double depletions of *hbl-1* and *lin-41* fully suppress both *lin-4* and *let-7* phenotypes, but neither single depletion is able to suppress any *lin-4* phenotypes or fully suppress the *let-7* mutant phenotypes (Abrahante et al., 2003).

Recently, it has been shown that the LIN-41 targets involved in the regulation of seam cell proliferation and differentiation are the EGR transcription factor *lin-29a* and *mab-10*, its NAB co-factor (Aeschimann et al., 2017, 2019). How the *lin29b* isoform is regulated is still unknown. This observation suggests that there could be a mechanism to separately regulate LIN-29a and LIN29b in different tissue and/or at different time points in development in order to allow the isoforms to exert a different function in the completion of the juvenile-to-adult transition.

1.4 Conservation of heterochronic genes in different species

Some members of the heterochronic pathway identified in *C. elegans* have homologs across different species, such as the miRNA gene *let-7* and genes related to *lin-28* and *lin-41*, which encode unique domain combinations. Others belong to conserved gene families, such as *lin-29* and *hbl-1*. Interestingly, it has been shown that not only the domain architectures of these regulators are conserved, but also their involvement in controlling self-renewal and differentiation of stem or progenitor cells. Moreover, in mammals these factors are interconnected in a conserved pathway: LIN-28 controls *let-7* processing, and *let-7* regulates LIN-41 expression trough mRNA degradation and translational repression. Thus, it seems possible that heterochronic genes have a conserved role in the regulation of developmental transitions and are involved in developmental timing in other animals.

1.4.1 *let-7* miRNA promote terminal differentiation

The *let-7* miRNAs family is highly conserved across animal species. The number of members of the family can differ between organisms. Except for *Drosophila melanogaster* that has only one *let-7*, *Danio rerio* has eleven members and mammals have ten miRNAs sharing the exact *let-7* seed sequence. It has been shown that let-7 has an important role in regulating cell proliferation and differentiation in different animals. Generally, the increase of *let-7* levels during late development is preserved in many organisms. Moreover, the genomic location and post-transcriptional regulation of the *let-7* family is similar in different animals (Roush and Slack, 2008).

In *Drosophila*, *let-7* levels increase during development with a peak at pupa, with an expression pattern that coincides with an ecdysone pulse. *let-7* regulates the timing

of differentiation of neuroblasts in the central nervous system and the formation of neuromuscular junctions in the abdominal muscles. *let-7* mutants show, on the one hand, juvenile type of neurons that didn't go through metamorphosis, and on the other, juvenile neuromuscular features into adulthood that lead to defects in flight, motility and fertility. Furthermore, *let-7* is required to stop proliferation of wing cells during metamorphosis. In the fruit fly, *let-7* exerts its functions through the downregulation of the *abrupt* gene to ensure proper neuronal morphogenesis, correct abdominal neuromusculature remodeling and cell cycle exit of the wing cells (Roush and Slack, 2008).

In vertebrates, *let-7* miRNAs family expression dramatically increases as cells become more differentiated. For example, increased levels of *let-7* are detected during metamorphosis of *Xenopus laevis*, at the embryo to larva transition of zebrafish and during embryonic stem cell (ECSs) differentiation and mouse development (Faunes and Larraín, 2016). Moreover, it has been shown that reduced expression of multiple *let-7* family members is associated with human cancers and with cancer stem cells, suggesting that this family of miRNAs promotes terminal differentiation in development and function as tumor suppressors (Roush and Slack, 2008).

1.4.2 The RBPs LIN28 and LIN41 promote stem cell proliferation

RNA binding proteins play an important role in proliferation and differentiation of stem cells and progenitor cells. In vertebrates, there are two paralogs of LIN-28, LIN28A and LIN28B. Both paralogs are expressed early in development in different species - zebrafish, *Xenopus* and mice (Moss and Tang, 2003; Yang and Moss, 2003). It has been shown that LIN-28 is important for organismal growth, metabolism and tissue development (Shyh-Chang and Daley, 2013). However, the function of LIN-28 during development of vertebrates is still under investigation.

LIN28 has an important role in stem cells differentiation and reprogramming. In fact, it has been shown that *lin-28* promotes, not only the self-renewal state of ESCs (Ye and Blelloch, 2014), but also that of multiple tissue lineages, including several cancer cell lines (Shyh-Chang and Daley, 2013). Moreover, it has been shown that LIN-28 expression increases the cell reprogramming efficiency of human fibroblast into induced pluripotent stem cells (iPSCs) (Yu et al., 2007). *lin-28* is also expressed during early neural development and in neural stem and progenitor cells (NSPCs), where its decrease is necessary for neuron-to-glia switch (Balzer et al., 2010). Interestingly, *lin-28* blocks the processing of *pri-let-7* in order to inhibit its

maturation in ESCs (Viswanathan et al., 2008), suggesting that the control of proliferation and differentiation of the axis *let-7/lin-28* is highly conserved from worms to mammals. Moreover, *lin-28* regulates the translation of several genes, including transcripts encoding cyclins, splicing factors, metabolic enzymes and ribosomal proteins. LIN-28 promotes translation of its targets, but the mechanism of this function remains unclear.

The other RNA binding protein of the *C. elegans* heterochronic pathway, *lin-41*, known as TRIM71 in vertebrates, is also a highly conserved regulator of self-renewal, differentiation, and cell fate plasticity. The mammalian LIN41 has two different functions. LIN41 function as a E3 ubiquitin ligase, ubiquitylating target proteins (Chen et al., 2013; Rybak et al., 2008) and as an RNA binding protein, repressing target mRNAs (Chang et al., 2012; Loedige et al., 2013; Welte et al., 2019; Worringer et al., 2014). Both activities have been proposed to be involved in promoting stem or progenitor cell proliferation (Chang et al., 2012; Chen et al., 2013; Rybak et al., 2008; Worringer et al., 2014). *lin-41* promotes cell proliferation of mouse and human embryonic stem cells and reprogramming of somatic cells in mammals (Chang et al., 2012; Rybak et al., 2008; Worringer et al., 2014). It is also reported that *lin-41* is involved in neural tube growth and closure and is essential for mouse development. Moreover, *lin-41* is important for neuronal development and plasticity, as it stimulates proliferation and inhibits premature differentiation of mouse neural progenitor cells (Chen et al., 2013; Cuevas et al., 2015).

1.4.3 Transcription factors regulating cell proliferation and differentiation: Krüppel family and Ikaros family

The LIN-28-*let-7*-LIN-41 module has been proposed to be a conserved control mechanism in stem cell development. However, also two heterochronic genes encoding for transcription factors, *lin-29* and *hbl-1*, belong to conserved gene families involved in the temporal regulation of cell proliferation and differentiation.

The nematode LIN-29 contains a domain conserved in Krüppel family early growth response (EGR) transcription factors, and *mab-10* encodes a NAB (NGFI-A-binding protein) transcriptional co-factor, known to bind to EGR proteins to regulate their activity (Harris and Horvitz, 2011). In mammals, there are four different EGR transcription factors, EGR1-4, and two NAB paralogs, NAB1 and NAB2. Interestingly, mammalian EGR proteins act with NAB proteins as transcriptional activators or repressors of genes that regulate proliferation and/or

terminal differentiation in different cell types: keratinocytes, chondrocytes, macrophages and Schwann cells (Du et al., 2014; Laslo et al., 2006; Le et al., 2005; Min et al., 2008; Nguyen et al., 1993; Topilko et al., 1994). For example, the reprogramming efficiency of fibroblasts into iPSCs is reduced by EGR1 (Worringer et al., 2014). EGR2 with NAB1/2 promotes terminal differentiation of the Schwann cells from promyelinating stage in myelinating stage (Le et al., 2005). Macrophage differentiation, instead, depends on expression of EGR1, EGR2 and NAB2. Interestingly, mutation in both NAB1 and NAB2 cause overproliferation of keratinocytes in mice (Le et al., 2005).

C. elegans hbl-1, instead, is related to *Drosophila Hunchback* and to Ikzf1/Ikaros family of zinc fingers transcription factors in mammals (Moss and Romer-Seibert, 2014). In the fly, *Hunchback* is essential for the specification of the anterior/posterior body axis, but also for differentiation of neuroblast precursors in neurons and glia of the central nerve cord. Neuroblasts undergo multiple rounds of asymmetric cell division to produce distinct neural type that are marked by the expression of four transcription factors, depending on when they are born. In particular, *Hunchback* is the first transcription factor to be expressed and its accumulation is necessary and sufficient to specify the temporal identity of early-born cells. *Krüppel* expression is the second one appearing and maintained in neurons generated later in time, which adopt second-born temporal identity (Kohwi and Doe, 2013; Moss and Romer-Seibert, 2014). When one of the transcription factors is lost, cells skip a specific temporal identity, instead constitutive expression of one of the factors causes repeated production of that specific cell type (Isshiki et al., 2001).

In mammals, Ikaros family members are widely expressed from embryo to adult and they have a crucial role in regulating cell-fate decisions during hematopoiesis, in particular in the development of the adaptive immune system. Ikaros is important for the balanced production of different blood and immune cells. It promotes on one side hematopoietic precursor self-renewal and on the other it functions as a key factor for differentiation at a number of branch points in the hematopoietic lineage (John and Ward, 2011). Moreover, Ikaros plays a role in neural development, promoting early fates in the retina and in the cortex. In the retina, Ikaros expression confers early temporal competence to retinal precursor cells such that they can generate early-born retinal cell types. When mis-expressed in later differentiated retinal precursors, it is sufficient to generate early-born neurons (Elliott et al., 2008). Ikaros is also expressed in early progenitor cells of the mouse cerebral cortex, where it

is sufficient to promote early cortical neuronal fates. If the expression of Ikaros is increased and sustained in the cortex, there is an increase in neural differentiation at early stages, a disrupted cortical structure and a displacement of progenitor cells within the cortical plate (Alsiö et al., 2015).

1.5 Motivation and aims for this thesis

The heterochronic pathway in *C. elegans* exemplifies a timing mechanism that involves coordination of multiple developmental events. Given the extensive evolutionary conservation of the heterochronic genes in controlling developmental transitions, it is of great interest to understand the molecular principles that drive such temporal coordination. Currently, the heterochronic pathway is described as a linear chain of events that leads to the upregulation of LIN-29. *let-7* silences LIN-41, and thereby relieves *lin-29* from translational repression by LIN-41 (Aeschimann et al., 2017; Faunes and Larraín, 2016; Moss and Romer-Seibert, 2014; Rougvie and Moss, 2013). Consequently, the accumulation of LIN-29 promotes the juvenile-to-adult transition events (Ambros and Horvitz, 1984; Bettinger et al., 1997).

However, several pieces of evidence suggest that the current model of J/A transition timing through *let-7*–LIN-41-mediated control of LIN-29 needs to be revised. Thus, LIN-29 occurs in two isoforms, LIN-29a and LIN-29b (Rougvie and Ambros, 1995), and LIN-41 only regulates *lin-29a* but not *lin-29b* (Aeschimann et al., 2017). Moreover, *let-7* mutations do not recapitulate all phenotypes of *lin-29(0)* (Ambros, 1989), and *let-7* appears to be dispensable for timing of seam cell fusion (Hunter et al., 2013). Finally, *lin-41(0)* mutant precocious phenotypes, unlike the retarded *lin-29(0)* mutant phenotypes, are only partially penetrant (Slack et al., 2000).

In this work, I therefore aim to address these discrepancies studying the involvement of LIN-29 isoforms in the regulation of different J/A transition events. After demonstrating that the J/A transition relies on two separate arms of the heterochronic pathway, defined by the regulation of the two *lin-29* isoforms, we defined an additional aim for this thesis. As our experiments revealed that *lin-29b* is regulated only by HBL-1 and not LIN-41, we aim to investigate the molecular function of a parallel arm of the heterochronic pathway centered on the Hunckback/Ikaros transcription factor HBL-1.

A better characterization of the mode of action of the heterochronic regulators will help, on the one hand, to shed light on the timing mechanism governing *C. elegans* development, on the other, to increase our knowledge about biological time-keeping in general.

2 Results

2.1 Publication: A branched heterochronic pathway directs juvenile-to-adult transition through two LIN-29 isoforms

C.A. conceived the project; designed, performed, and analyzed confocal microscopy, luciferase assay, RT-qPCR and western blot experiments; created transgenic worm lines; and wrote, reviewed and edited the manuscript. F.A. conceived the project; designed, performed, and analyzed confocal microscopy, phenotypic analysis and western blot experiments; created transgenic worm lines; and reviewed and edited the manuscript. A.N. performed and analyzed the precious expression experiment; and created transgenic worm lines. H.G. conceived the project; designed and analyzed experiments; acquired funding; and wrote, reviewed and edited the manuscript.

2.1.1 Figures supplement

genotype	LIN-29a activity	LIN-29b activity	J/A transition events (black = normal, red = abnormal)
wt	MAB-10 / LIN-29a → promoter → target genes	MAB-10 / LIN-29b → promoter → target genes	seam cell fusion seam cell cycle exit alae formation molting stop
mab-10(0)	LIN-29a → promoter → target genes	LIN-29b → promoter → target genes	seam cell fusion seam cell cycle exit alae formation molting stop
lin-29a(Δ)	promoter → target genes	MAB-10 / LIN-29b → promoter → target genes	seam cell fusion seam cell cycle exit alae formation molting stop
mab-10(0) lin-29a(Δ)	promoter → target genes	LIN-29b → promoter → target genes	seam cell fusion seam cell cycle exit alae formation molting stop
lin-29b(Δ) or lin-29b(lf)	MAB-10 / LIN-29a → promoter → target genes	promoter → target genes	seam cell fusion seam cell cycle exit alae formation molting stop
mab-10(0) lin-29b(Δ) or lin-29b(lf)	LIN-29a → promoter → target genes	promoter → target genes	seam cell fusion seam cell cycle exit alae formation molting stop
lin-29ab(Δ)	promoter → target genes	promoter → target genes	seam cell fusion seam cell cycle exit alae formation molting stop

Figure 6–figure supplement 1: Summary of phenotypes of mutant animals examined in this study

Summary of the J/A transition phenotypes seen for different permutations of *lin-29a*, *lin-29b*, and *mab-10* mutations. Note that extra seam cell divisions in *mab-10(0)* mutant animals occur only in older adults. Some older *mab-10* mutant adults may also undergo extra molts (Harris and Horvitz, 2011), although we did not observe this.
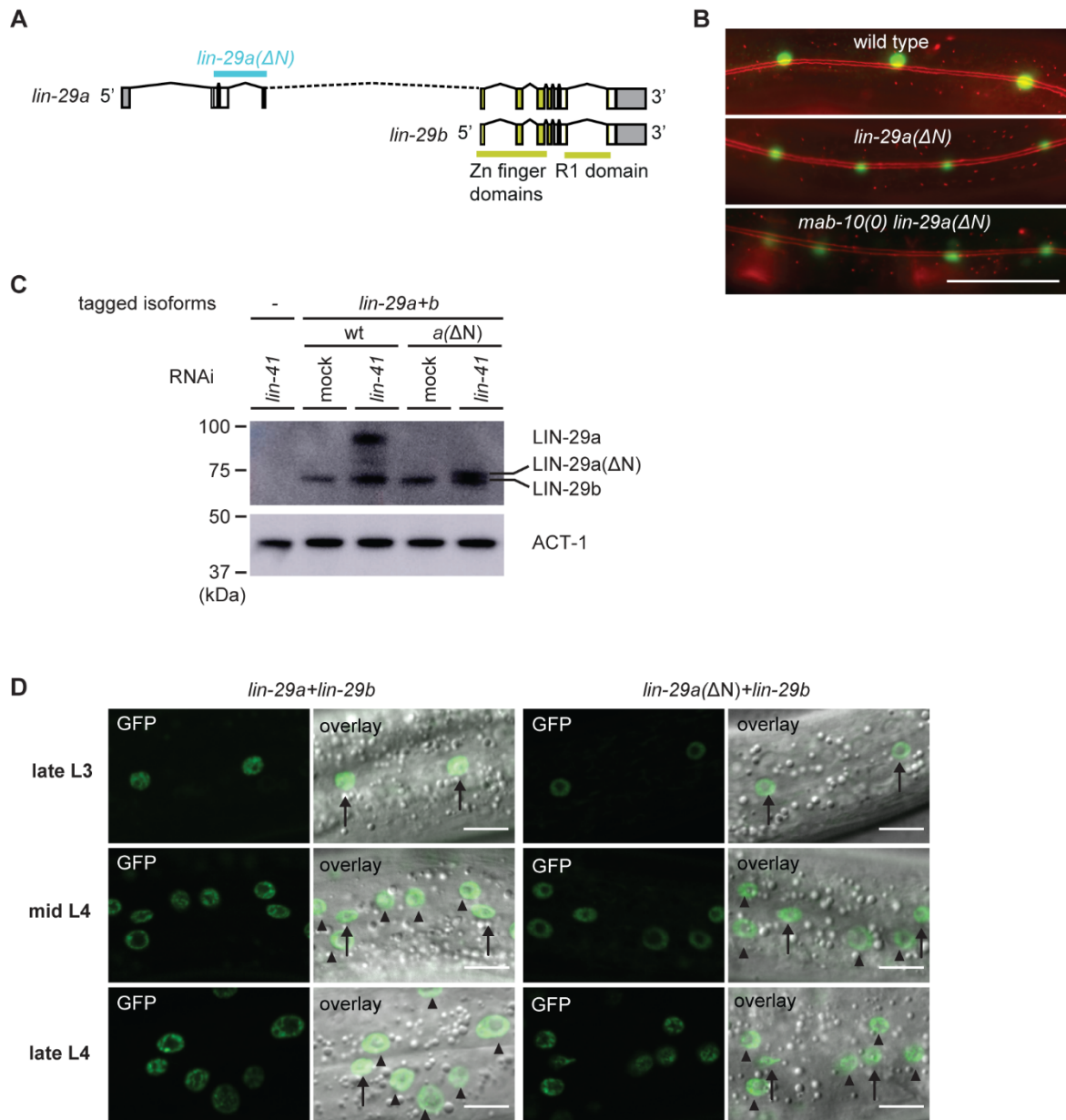
Figure 6–figure supplement 2: Characterization of *lin-29a(ΔN)* expression and function

(A) Schematic representation of the *lin-29a(ΔN)* deletion.

(B) Micrographs of late L4-stage animals of indicated genotypes expressing *scm::gfp* (*green*, marking seam cells) and *ajm-1::mCherry* (*red*, marking hypodermal cell junctions). In both *lin-29a(ΔN)* and *mab-10(0) lin-29a(ΔN)* animals, fusion occurs normally. Scale bar: 50 μm.

(C) Western blot of C-terminally GFP::3xFLAG-tagged endogenous LIN-29a and LIN-29b proteins in a wild-type and the *lin-29a(ΔN)* background (HW2408), respectively, using anti-FLAG antibody. Animals were grown for 20 h at 25°C to the L3 stage on mock RNAi and *lin-41*

RNAi bacteria, respectively. Both LIN-29a and LIN-29a(ΔN) accumulate upon knock-down of *lin-41.* Actin-1 is used as a loading control.

(D) Confocal images of endogenously tagged LIN-29 protein isoforms in the wild type and *lin-29a(ΔN)* background (HW2408) in the epidermis of animals at the indicated developmental stages. Animals were staged by examination of gonad development. Arrows indicate seam cell, arrowheads hyp7 nuclei. Scale bars: 10 μm.
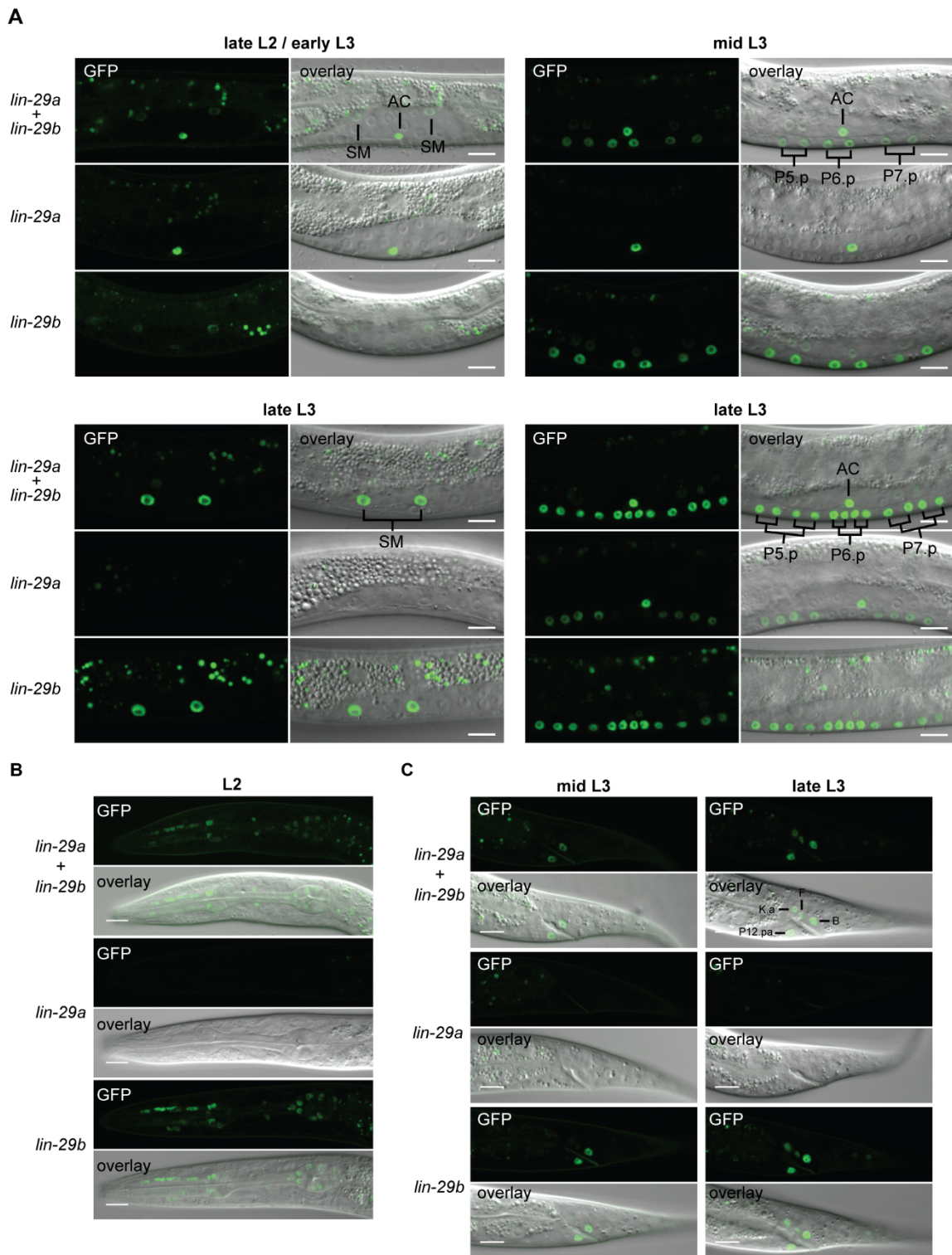
Figure 7–figure supplement 1: Expression of *lin-29* isoforms

(A) Confocal images of endogenously tagged LIN-29 protein isoforms in the region of the vulva and the uterus at the indicated developmental stages. At the L2-to-L3 molt (A), *lin-29a* is expressed in the anchor cell (AC), while *lin-29b* is weakly expressed in the sex myoblasts (SMs).

In mid-L3 stage worms, the six daughters of the VPCs P5.p-P7.p express *lin-29b.* At the late L3 stage, *lin-29b* is strongly expressed in the sex myoblast (SM) daughters and all 12 granddaughters of the VPCs P5.p-P7.p, while LIN-29a specifically accumulates in the granddaughters of P5.p and P7.p, but not in those of P6.p. Scale bars: 10 μm.

(B) Confocal images of endogenously tagged LIN-29 protein isoforms in the pharynx of L2 stage animals at the indicated developmental stages. *lin-29b* but not *lin-29a* is expressed in the pharynx throughout larval and adult development. Scale bars: 10 μm.

(C) Confocal images of endogenously tagged LIN-29 protein isoforms in the tail region at the indicated developmental stages. LIN-29b first accumulates in the two rectal cells B and P12.pa, before accumulating in the four additional rectal cells F, K.a, K' and U (B, the latter two are not visible in this focal plane). LIN-29a is not detected in these cells. Scale bars: 10 μm.
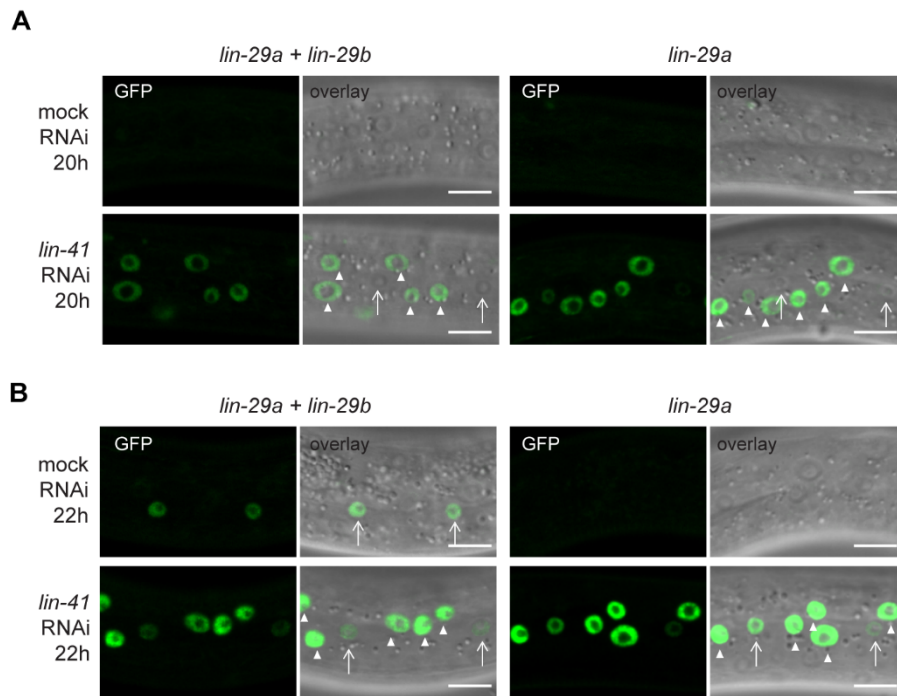
Figure 9–figure supplement 1: Expression of *lin-29a* on *lin-41* RNAi over time

(A-B) Confocal images of endogenously tagged LIN-29 protein isoforms in the epidermis (strains HW1822, HW1826, HW1835). Animals were grown at 25°C for 20 h (A) or 22h (B) on RNAi bacteria as indicated. Arrows indicate seam cell, arrowheads hyp7 nuclei. Scale bars: 10 µm.
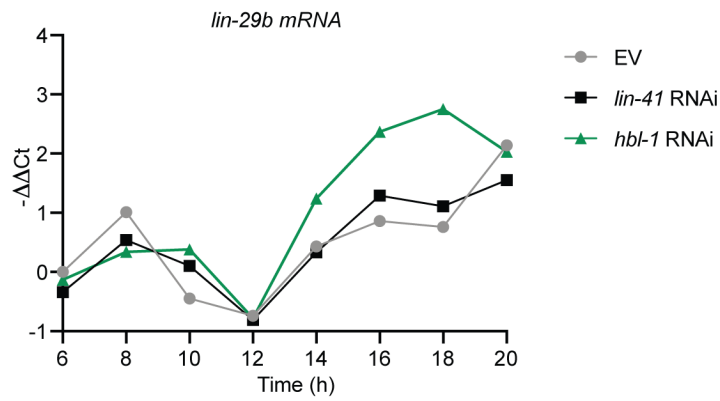
Figure 9–figure supplement 2: mRNA levels of lin-29b on *lin-41* and *hbl-1* RNAi worms over time

RT-qPCR analysis to measure the -ΔΔCt of *lin-29b* mRNA levels (normalized by *act-1* mRNA levels) over time. Wild-type animals exposed to *lin-41* and *hbl-1* RNAi compared to mock RNAi.
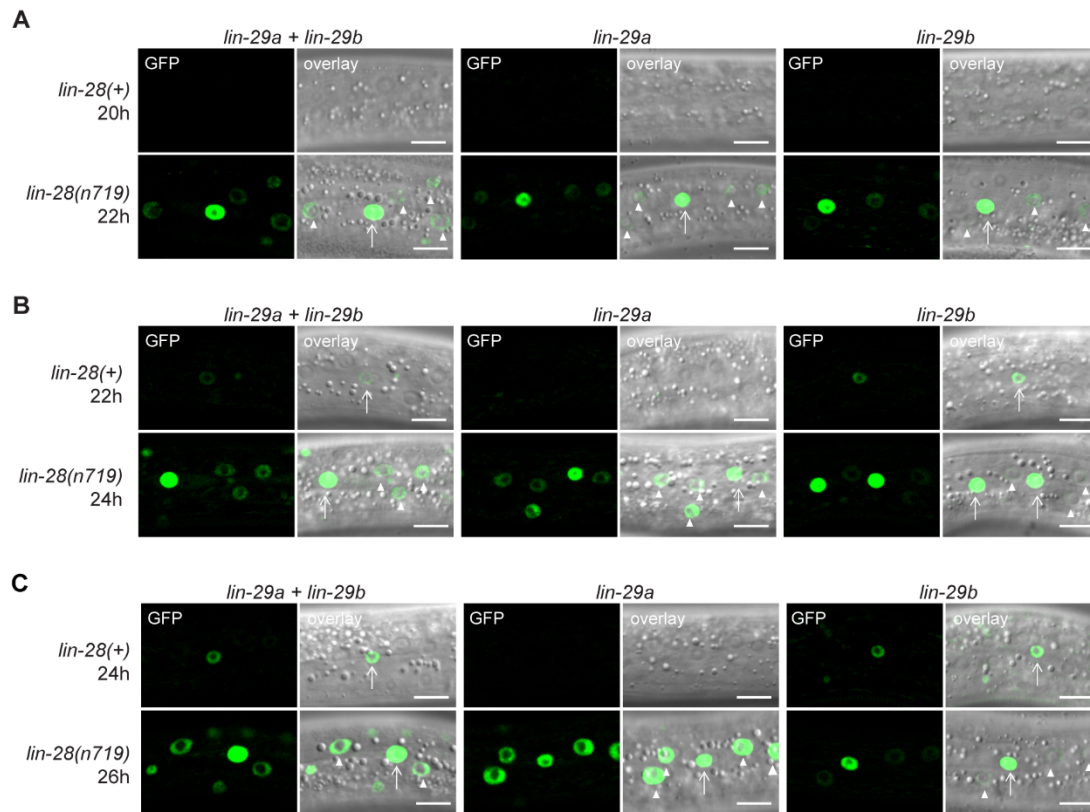
Figure 10–figure supplement 1: mRNA levels of lin-29b on *lin-41* and *hbl-1* RNAi worms over time

(A-C) Confocal images of endogenously tagged LIN-29 protein isoforms in wild-type (*lin-29(+)*) or *lin-28(n719)* background in the epidermis (strains HW1822, HW1826, HW1835, HW1924, HW1925, HW1926). Animals were grown at 25°C for 20 h, 22 h and 24 h (A, B, and C, resp., for control strains) and 22 h, 24 h and 26 h (A, B, and C, resp., for *lin-28(n719)* strains) to reach an equivalent developmental stage. Arrows indicate seam cell, arrowheads hyp7 nuclei. Scale bars: 10 μm.

2.1.2 Source data

Figure 1—source data 1

Quantification of unfused seam cell junctions, raw data related to Figure 1B.

Stage: late L4			
worm line with ajm marker	completely fused	not fused	total number of counted worms
N2 (wild-type)	34	0	34
let-7(n2853)	24	0	24
let-7(xe150)	57	0	57
lin-41(xe8)	34	0	34

Figure 3—source data 1

Quantification of unfused seam cell junctions, raw data related to Figure 3C.

Stage: late L4	completely fused	unfused junction = uj														total number of counted worms
worm line with ajm marker		1 uj	2 uj	3 uj	4 uj	5 uj	6 uj	7 uj	8 uj	9 uj	10 uj	11 uj	12 uj	13 uj	14 uj	
N2 (wild-type)	22	0	0	0	0	0	0	0	0	0	0	0	0	0	0	22
lin-29(xe40)	22	0	0	0	0	0	0	0	0	0	0	0	0	0	0	22
lin-29(xe116)	0	0	2	1	1	5	1	6	3	4	1	2	5	0	0	31
lin-29(xe120)	0	0	0	0	0	1	2	1	3	3	11	5	6	0	0	32
mab-10(xe44)	22	0	0	0	0	0	0	0	0	0	0	0	0	0	0	22
mab-10(xe44) lin-29(xe40)	22	0	0	0	0	0	0	0	0	0	0	0	0	0	0	22
mab-10(xe44) lin-29(xe116)	0	0	0	2	4	3	7	5	1	5	3	2	0	0	0	32
mab-10(xe44) lin-29(xe120)	0	0	0	0	0	2	6	5	5	4	2	5	1	0	0	30
lin-29(xe37)	0	0	0	0	0	0	0	0	1	1	5	4	5	10	5	31

Figure 3—source data 2

Quantification of unfused seam cell junctions, raw data related to Figure 3B.

Stage: young Adult	completely fused	unfused junction = uj									total number of counted worms
worm line with ajm marker		1 uj	2 uj	3 uj	4 uj	5 uj	6 uj	7 uj	8 uj	>8 uj	
N2 (wild-type)	18	0	0	0	0	0	0	0	0	0	18
lin-29(xe40)	36	0	0	0	0	0	0	0	0	0	36
mab-10(xe44)	38	0	0	0	0	0	0	0	0	0	38
mab-10(xe44) lin-29(xe40)	14	0	0	0	0	1	0	0	1	13	29
lin-29(xe37)	0	0	0	0	0	0	0	0	0	40	40

Figure 3—source data 3

Quantification of seam cell numbers, raw data related to Figure 3D.

Stage: late L4	number of seam cells																		total number of counted worms
worm line with scm marker	15	16	17	18	19	20	21	22	23	24	25	26	27	28	29	30	31	32	
N2 (wild-type)	1	13	8	0	0	0	0	0	0	0	0	0	0	0	0	0	0	0	22
lin-29(xe40)	0	17	5	0	0	0	0	0	0	0	0	0	0	0	0	0	0	0	22
lin-29(xe116)	1	24	6	0	0	0	0	0	0	0	0	0	0	0	0	0	0	0	31
lin-29(xe120)	1	27	4	0	0	0	0	0	0	0	0	0	0	0	0	0	0	0	32
mab-10(xe44)	0	16	5	1	0	0	0	0	0	0	0	0	0	0	0	0	0	0	22
mab-10(xe44) lin-29(xe40)	0	17	5	0	0	0	0	0	0	0	0	0	0	0	0	0	0	0	22
mab-10(xe44) lin-29(xe116)	1	25	5	1	0	0	0	0	0	0	0	0	0	0	0	0	0	0	32
mab-10(xe44) lin-29(xe120)	1	21	6	2	0	0	0	0	0	0	0	0	0	0	0	0	0	0	30
lin-29(xe37)	0	27	4	0	0	0	0	0	0	0	0	0	0	0	0	0	0	0	31
mab-10(xe44) lin-29(xe37)	0	17	3	0	0	0	0	0	0	0	0	0	0	0	0	0	0	0	20

Stage: young adult	number of seam cells																		total number of counted worms
worm line with scm marker	15	16	17	18	19	20	21	22	23	24	25	26	27	28	29	30	31	32	
N2 (wild-type)	1	33	18	3	0	0	0	0	0	0	0	0	0	0	0	0	0	0	55
lin-29(xe40)	1	37	12	3	0	0	0	0	0	0	0	0	0	0	0	0	0	0	53
lin-29(xe116)	0	7	9	8	6	7	11	7	2	2	0	1	0	1	0	0	0	0	61
lin-29(xe120)	0	0	0	0	0	0	0	0	0	8	13	12	7	9	3	0	0	0	52
mab-10(xe44)	1	36	12	4	0	0	0	0	0	0	0	0	0	0	0	0	0	0	53
mab-10(xe44) lin-29(xe40)	0	14	8	3	0	1	1	0	0	3	6	8	3	2	2	0	1	0	52
mab-10(xe44) lin-29(xe116)	0	0	0	1	1	0	0	2	1	4	8	11	12	5	3	1	2	0	51
mab-10(xe44) lin-29(xe120)	0	0	0	0	0	0	0	0	0	1	8	12	11	9	7	3	0	0	51
lin-29(xe37)	0	0	0	0	0	0	0	0	0	2	8	7	13	13	3	4	2	0	52
mab-10(xe44) lin-29(xe37)	0	0	0	0	0	0	0	0	0	3	6	12	13	9	3	2	4	0	52

Figure 4—source data 1

Quantification of alae structures, raw data related to Figure 4B.

Stage: young adult							
worm line	complete alae	complete weak alae	partial weak alae >= 50%	partial weak alae <50%	alae patches (1-4)	absent alae	number of scored worms
N2 (wild-type)	32	0	0	0	0	0	32
lin-29(xe40)	0	21	12	0	0	0	33
lin-29(xe116)	0	0	0	0	31	2	33
lin-29(xe120)	0	0	0	0	19	14	33
mab-10(xe44)	32	0	0	0	0	0	32
mab-10(xe44) lin-29(xe40)	0	19	15	0	0	0	34
mab-10(xe44) lin-29(xe116)	0	0	0	0	31	2	33
mab-10(xe44) lin-29(xe120)	0	0	0	0	17	16	33
lin-29(xe37)	0	0	0	0	0	32	32

Figure 5—source data 1

Quantification of number of molts, raw data related to Figure 5B.

worm line	4 molts	5 molts	6 molts	total number of worms
N2 (wild-type)	336	0	0	336
lin-29(xe40)	96	0	0	96
lin-29(xe116)	112	0	0	112
lin-29(xe120)	94	0	0	94
mab-10(xe44)	105	0	0	105
mab-10(xe44) lin-29(xe40)	50	10	6	66
mab-10(xe44) lin-29(xe116)	125	0	0	125
mab-10(xe44) lin-29(xe120)	28	0	0	28
lin-29(xe37)	0	144	124	268

Figure 6—source data 1

Quantification of seam cell numbers, raw data related to Figure 6B.

Stage: late L4																		
	number of seam cells																	total number of counted worms
worm line with scm marker	15	16	17	18	19	20	21	22	23	24	25	26	27	28	29	30	31	32	
N2 (wild-type)	4	42	22	1	0	0	0	0	0	0	0	0	0	0	0	0	0	0	69
lin-29(xe200)	0	45	12	5	2	0	0	0	0	0	0	0	0	0	0	0	0	0	64
mab-10(0) lin-29(xe200)	3	32	13	2	0	0	0	0	0	0	0	0	0	0	0	0	0	0	50
lin-29(xe37)	0	19	7	2	0	0	0	0	0	0	0	0	0	0	0	0	0	0	28
Stage: young adult																			
	number of seam cells																		total number of counted worms
worm line with scm marker	15	16	17	18	19	20	21	22	23	24	25	26	27	28	29	30	31	32	
N2 (wild-type)	0	31	14	3	0	0	0	0	0	0	0	0	0	0	0	0	0	0	48
lin-29(xe200)	0	24	13	2	0	0	0	0	0	0	0	0	0	0	0	0	0	0	39
mab-10(0) lin-29(xe200)	0	19	14	5	0	0	0	0	0	0	0	0	0	0	0	0	0	0	38
lin-29(xe37)	0	0	0	2	0	3	2	1	1	3	2	5	1	2	2	1	1	0	26

Figure 6—source data 2

Quantification of alae structures, raw data related to Figure 6C.

Stage: young adult							
worm line	complete alae	complete weak alae	partial weak alae >= 50%	partial weak alae <50%	alae patches (1-4)	absent alae	number of scored worms
N2 (wild-type)	52	0	0	0	0	0	52
Lin-29(xe200)	39	0	0	0	0	0	39
mab-10(xe44)lin-29(xe200)	31	0	0	0	0	0	31
Lin-29(xe37)	0	0	0	0	0	28	28

Figure 6—source data 3

Quantification of number of molts, raw data related to Figure 6D.

worm line	4 molts	5 molts	6 molts	total number of worms
N2 (wild-type)	116	0	0	116
lin-29(xe200)	351	0	0	351
mab-10(xe44) lin-29(xe200)	305	0	0	305
lin-29(xe37)	0	37	42	79

Figure 6—figure supplement 2—source data 1

Quantification of unfused seam cell junctions, raw data related to Figure 6—figure supplement 2B.

Stage: late L4				
worm line with ajm marker	completely fused	not fused	1 uj	total number of counted worms
N2 (wild-type)	68	0	1	69
lin-29(xe200)	64	0	0	64
mab-10(xe44) lin-29(xe200)	48	0	2	50
lin-29(xe37)	0	28	0	28

2.1.3 Supplementary files

Supplementary file 1A: Plasmids used in this study.

Short name	Plasmid backbone	Insert	Cloning technique	Primers[a] or gBlocks[b]	
pIK155	published in (Katic et al., 2015)				
pIK198	published in (Katic et al., 2015)				
pCFJ90	published in (Frøkjær-Jensen et al., 2008)				
pCFJ104	published in (Frøkjær-Jensen et al., 2008)				
pFA27	published in (Aeschimann et al., 2019)				
pFA224	pENTR L4-R1	*col-10* promoter		gift from Matyas Ecsedi. The col-10 promoter starts is 1320 bp long and starts with the following sequence: 5'-CCTCGGGTGGTCATCATCTCAAATTCCAATCTTCTTTTTCATTTTCAATCTCTAACAATTTCAAATTACTAGAACCCACAAACCAATGTTCGATA … – 3'	
pFA198	pENTR L1-L2	3xFLAG tag followed by BamHI restriction site (can be used for Gibson assembly instead of BP reaction)	BP reaction[c]	fwd primer	ggggacaagtttgtacaaaaaagcaggctATGGATTATAAAGACGATGACGATAAGCGTGA
				rev primer	ggggaccactttgtacaagaaagctgggtGGATCCTCTCTTGTCATCGTCATCCTTGTAATC
pFA199	pENTR L1-L2	3xFLAG::*lin-29a* (ORF and 3'UTR; including introns except for intron 4)	Gibson assembly[d]	fwd(1)	acaaggatgacgatgacaagagaATGGATCAAACTGTTCTAGATTCGGCA
				rev(1)	gcttttgttcgaaCTGTGGATATCTTCCAAATTGTGA
				fwd(2)	tggaagatatccacagTTCGAACAAAAGCCGGACGT
				rev(2)	tgcccactttgtacaagaaagctgggtCCACTGTGCATGAAAAAGCTGGT
pFA206	pENTR L1-L2	3xFLAG::*lin-29b* (ORF and 3'UTR, including introns)	Gibson assembly[e]	fwd primer	acaaggatgacgatgacaagagaATGCAGATGCGGGAAGCAAAAC
				rev primer	tgcccactttgtacaagaaagctgggtCCACTGTGCATGAAAAAGCTGGT
pFA207	pENTR L1-L2	3xFLAG::*mab-10* (ORF and 3'UTR, including introns)	Gibson assembly[e]	fwd primer	acaaggatgacgatgacaagagaATGTCATCATCGTCGTCGTC
				rev primer	tgcccactttgtacaagaaagctgggtACTATTGTTACGGGAATCATGTCT
pFA218	published in (Aeschimann et al., 2019)				
pFA219	pENTR L1-L2	FLAG-HA-degron::*lin-29a* (ORF and 3'UTR; including introns except for intron 4)	Gibson assembly[f]	fwd primer	aggcggcggcgttcgtgaagATGGATCAAACTGTTCTAGATTCGGCA
				rev primer	tgcccactttgtacaagaaagctgggtCCACTGTGCATGAAAAAGCTGGT
pFA220	pENTR L1-L2	FLAG-HA-degron::*lin-29b* (ORF and 3'UTR, including introns)	Gibson assembly[f]	fwd primer	aggcggcggcgttcgtgaagATGCAGATGCGGGAAGCAAAAC
				rev primer	tgcccactttgtacaagaaagctgggtCCACTGTGCATGAAAAAGCTGGT
pFA221	pENTR L1-L2	FLAG-HA-degron::*mab-10* (ORF and 3'UTR, including introns)	Gibson assembly[f]	fwd primer	aggcggcggcgttcgtgaagATGTCATCATCGTCGTCGTC
				rev primer	tgcccactttgtacaagaaagctgggtACTATTGTTACGGGAATCATGTCT
pENTR_R2-L3_operon-GFP-H2b	published in (Ecsedi et al., 2015) based on (Merritt et al., 2008)				
pFA238	pCFJ150	pFA224, pFA219, pENTR_R2-L3_operon-GFP-H2b	LR reaction		
pFA239	pCFJ150	pFA224, pFA220, pENTR_R2-L3_operon-GFP-H2b	LR reaction		
pFA240	pCFJ150	pFA224, pFA221, pENTR_R2-L3_operon-GFP-H2b	LR reaction		

[a]Overhangs are in lowercase, the part annealing to the template in uppercase. If not stated otherwise, the PCR products were amplified from *C. elegans* genomic DNA.
[b]Overhangs for Gibson assembly reactions are in lowercase.
[c]PCR product was amplified from pFA27.
[d]Assembly with BamHI-digested plasmid pFA198 and two PCR products.
[e]Assembly with BamHI-digested plasmid pFA198 and one PCR product.
[f]Assembly with BamHI-digested plasmid pFA218 and one PCR product.

Supplementary file 1B: oligonucleotides and sgRNAs used in this study

Identifier	Sequence	Source	Description
CA1-2	ctaagcctaagtctatgcctaagcccaagcttgatctcacaatttaagctttcaaactagtgctaattaaag ggaatacggtttcagaattaaggagacacctagatcaattgagctctaaagatccactatattcaatgtac ttacagttcgaacaaaagccggacgtgggggtgcttcagcaacagatgcagatgcgg	This study	HR oligo for generation *lin-29(xe61 xe114)* and *lin-29(xe116)*
FA419	gaacggaatgatccgaaacctagatcaattgagctctaaagatccactatattcaatgtacttacagttc gaacaaaagccagatgtcggggtgcttcagcaacagatgcagatgcgggaagcaaaaccttacaagtgcacgcagtgtgtcaaggtatgtggt	This study	HR oligo for generation *lin-29(xe61 xe121)* and *lin-29(xe120)*

FA434	cctttcagcttcgcgaggatcaagccaacttcttcaacgcaatgtt ttcacaatttggaagatatccacag gtttgcatagggaacacattcaaacgagggtga	This study	HR oligo for generation *lin-29(xe61 xe133)* and *lin-29(xe200)*
3-AC15-16	acagaattaaggagacaagg	This study	sgRNA for generation *lin-29(xe61 xe114)* and *lin-29(xe116)*
2-AC2-3	agctcaattgatctaggtttt	This study (Aeschimann et al., 2019)	sgRNA for generation *lin-29(xe61 xe114)* and *lin-29(xe116)*
L29_ATG1	gttcgaacaaaagccggacg	(Aeschimann et al., 2019)	sgRNA for generation *lin-29(xe61 xe121)* and *lin-29(xe120)*
L29_ATG3	agctgaagcacccccacgtc	This study (Aeschimann et al., 2019)	sgRNA for generation *lin-29(xe61 xe121)* and *lin-29(xe120)*
L29_031	gctggaaccaccactggctc	This study (Aeschimann et al., 2019)	sgRNA for generation *lin-29(xe61 xe133)* and *lin-29(xe200)*
L29_041	gtggcaggagagaattctga	This study (Aeschimann et al., 2019)	sgRNA for generation *lin-29(xe61 xe133)* and *lin-29(xe200)*
L29_if1	agccaacttcttcaacgcaa	This study (Aeschimann et al., 2019)	sgRNA for generation *lin-29(xe61 xe133)* and *lin-29(xe200)*
L29_if3	gtgaaaacatatgatgtggc	This study (Aeschimann et al., 2019)	sgRNA for generation *lin-29(xe61 xe133)* and *lin-29(xe200)*
lin-29_F4	ccagcacatcattcgatcact	(Aeschimann et al., 2017)	qPCR primer for *lin-29a* specific detection (exon3-exon4 junction)
lin-29_R4	gaagttcagtagatccgcttga	This study (Aeschimann et al., 2019)	qPCR primer for *lin-29a* specific detection (exon3-exon4 junction)
lin-29_F5	acccaagtttgagttcgaaca	(Aeschimann et al., 2017)	qPCR primer for *lin-29b* specific detection (SL1-exon5 junction)
lin-29_R5	gatgagttggcaaatgccttga	(Aeschimann et al., 2017) This study (Aeschimann et al., 2019)	qPCR primer for *lin-29b* specific detection (SL1-exon5 junction)
JKq17	gtcggaagaccacgtcatcaa	This study (Aeschimann et al., 2019)	qPCR primer for *act-1* specific detection (exon1)

JKq18	agggtaaggatacctctcttgga	This study (Aeschimann et al., 2019)	qPCR primer for *act-1* specific detection (exon1-exon3 junction)

2.2 Characterization of a parallel arm of the heterochronic pathway centred on the transcription factor HBL-1

Chiara Azzi conceived the project; designed, performed, and analyzed confocal microscopy, luciferase assay, RNA sample collection; created transgenic worm lines. Dimos Gaidatzis and Milou Meeuse analyzed the mRNA-Seq data. Kathrin Braun created transgenic worm lines. Helge Grosshans conceived the project; designed and analyzed experiments.

Our work demonstrates that the J/A transition events in *C. elegans* rely on two separate arms of the heterochronic pathway. We showed that LIN-29 isoforms have partially distinct function in regulating the J/A transition events and thus functional specialization derives from distinct isoform expression pattern. The unique spatiotemporal expression of the two isoforms are the result of isoform-specific regulation: whereas *lin-29a* is regulated by LIN-41, the *lin-29b* isoform is regulated by the transcription factor HBL-1. The regulation of only *lin-29b* by HBL-1 is consistent with previous observations that *hbl-1(rf)* mutant animals show precocious seam cell fusion but not cessation of seam cell self-renewal (Abrahante et al., 2003; Lin et al., 2003), since, according to our data, the seam cell exit from cell cycle requires both *lin-29* isoforms. However, it is unknown how *lin-29b* regulation is achieved, and whether HBL-1 acts directly or indirectly on this isoform. Hence, to better understand the timing mechanism that underlies *C. elegans* development, we are interested in studying the placement of HBL-1 in the heterochronic pathway, its functions and its targets, and the mechanisms of *lin-29b* regulation.

2.2.1 Expression analysis of HBL-1

Available data on *hbl-1* expression pattern are difficult to interpret since they do not match the observed phenotype. For example, *hbl-1::gfp* multicopy array expression is not detected in seam cells at the L2 stage, while, by a genetic experiment, it has been shown that *hbl-1* regulates the symmetric seam cell division at this stage (Abbott, 2011).

In order to better characterize the expression pattern of *hbl-1*, we tagged HBL-1 at the endogenous locus with GFP using CRISPR-Cas9-mediated genome editing (Dokshin et al., 2018). We placed the tag at the N-terminus of HBL-1 to not interfere with the zinc finger domains, important for its activity as transcription factor, and to tag both reported isoforms (Figure 2.1A). We used confocal imaging of immobilized *gfp::hbl-1* animals to detect nuclear accumulation of GFP over development in different tissues. As already reported, HBL-1 is

expressed both embryonically and post-embryonically (Fay et al., 1999). Due to the important function of HBL-1 in the regulation of seam cells fate, we first observed the protein accumulation over development in the epidermis. We found that epidermal nuclear GFP signal is detectable in the L1 stage. HBL-1 accumulates in the hypodermal syncytial cells, hyp7, in the seam cells, and in the ventral hypodermal P cell. *hbl-1* expression stays high in these compartments until the L2 stage. By the early L3 stage, HBL-1 is not detected anymore in the seam cells, but it is still detected in the P cell descendents and weakly in the hyp7. By the mid-L3 stage, *hbl-1* is no longer expressed in the hyp7 and Pn.p cell descendants either (Figure 2.1B-C). HBL-1 is also clearly accumulated in tissues other than the epidermis. We observed accumulation of HBL-1 in the ventral nerve cord (VNC), where the signal is detectable from the L1 stage and downregulated by the end of the L3 stage (Figure 2.1D), and in the intestine, where the accumulation of HBL-1 is sustained during all larval stages (Figure 2.1D). Moreover, *hbl-1* is expressed in several other neurons in particular in the tail and in the head region and in some muscle cells (data not shown).
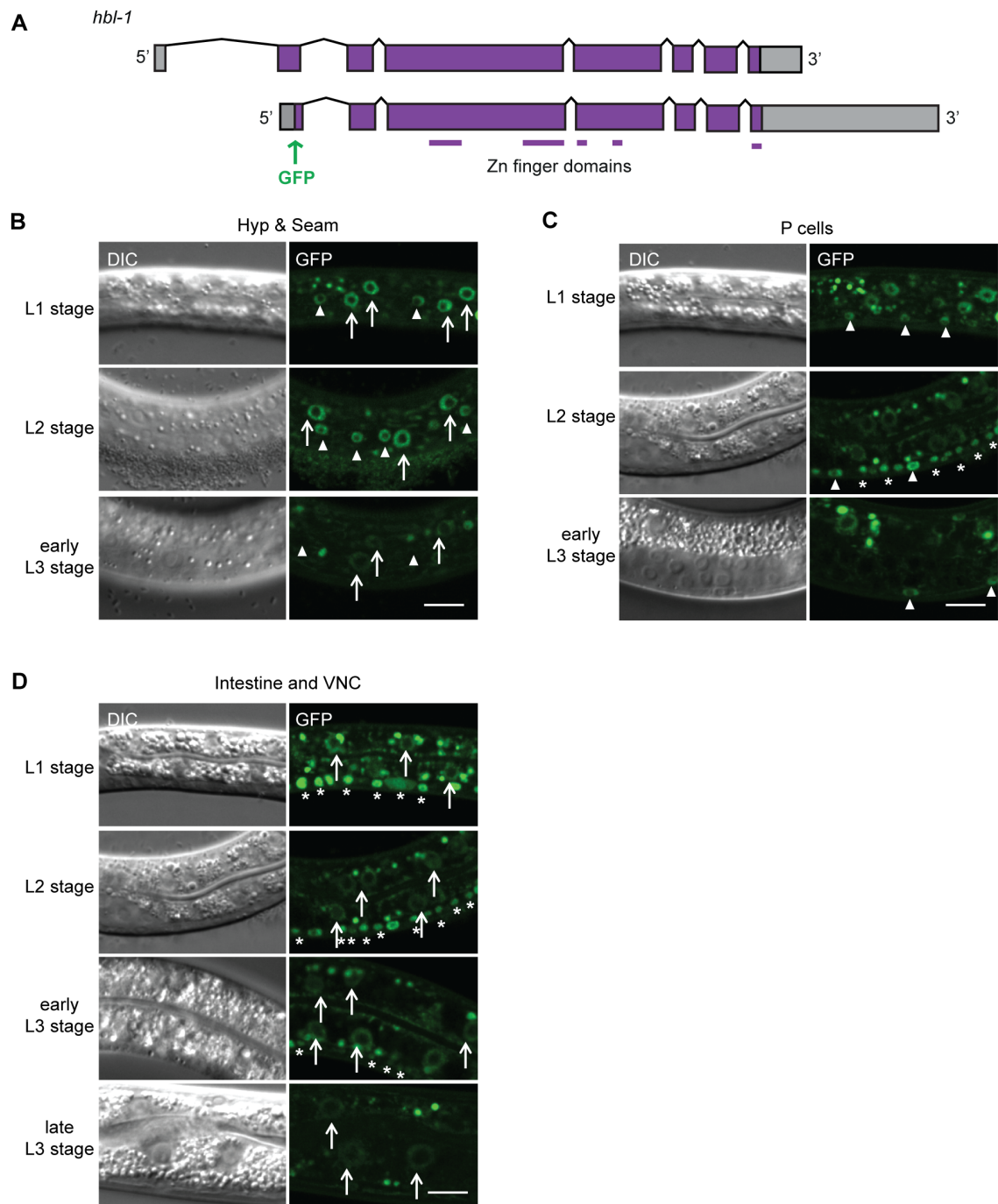
Figure 2.1 *hbl-1* is expressed in epidermis, VNC and intestine until the L3 stage

(A) Schematic representation of the *hbl-1* genomic region. Insertion of *gfp*-encoding sequence at the 5' end specifically tags HBL-1.

(B) Confocal images of endogenously GFP-tagged HBL-1 protein isoforms in seam cells and hyp7. Animals were grown at 25°C for 8h (L1 stage), 15h (L2 stage) and 20h (early L3 stage). Arrowhead indicate seam cell, arrow hyp7 nuclei. Scale bars: 10 μm.

(C) Confocal images of endogenously GFP tagged HBL-1 protein isoforms in the P cells and in the VNC. Animals were grown at 25°C for 8h (L1 stage), 15h (L2 stage) and 20h (early L3 stage). Arrowheads indicate P cells, asterisks indicate VNC. Scale bars: 10 μm.

(D) Confocal images of endogenously GFP-tagged HBL-1 protein isoforms in the VNC and intestine. Animals were grown at 25°C for 8h (L1 stage), 15h (L2 stage), 20h (early L3 stage) and 25h (late L3 stage). Asterisk indicate VNC, arrow indicate intestine nuclei. Scale bars: 10 μm.

2.2.2 Extensive depletion of HBL-1 causes a fully penetrant precocious exit from the molting cycle

We complemented the expression analysis with functional analysis. Since *hbl-1(0)* mutants died as embryos (Fay et al., 1999), we used the auxin inducible degradation (AID) system (Zhang et al., 2015) to deplete HBL-1 in a temporally controlled manner. To this end, we tagged *hbl-1* endogenously with *gfp::degron::3xflag*, and expressed the plant specific F-box protein TIR1 as a transgene (Figure 2.2A). In the presence of the plant hormone auxin, we observed rapid degradation of HBL-1, since after 1 hour we could not detect the GFP signal anymore (data not shown). When we plated synchronized L1 *gfp::degron::3xflag::hbl-1* animals on auxin-containing plates, we observed a penetrant Egl and Pvl phenotype, consistent with a previous report (Fay et al., 1999).

To understand the role of HBL-1 in regulation the J/A transition, we tested its involvement in the molting cycle exit. We used the luciferase assay, a high throughput method that allows us to score defects in the termination of the molting cycle by monitoring the development of individuals animals (Meeuse et al., 2020; Olmedo et al., 2015). In the luciferase assay, the worms, expressing luciferase from a ubiquitously and constitutively active *eft-3* promoter, are synchronized and then cultured in the presence of luciferin, the luciferase substrate, in a temperature-controlled luminometer. The luminescent signal increases throughout development, but drops during lethargus, when the worms stop eating and go through the molt. This reduction of luminescence followed by the rebound of the signal allows to describe defects in the exit from the molting cycle, revealing abnormal number of molts.

We took advantage of the *gfp::degron::3xflag::hbl-1* animals, expressing TIR1 and luciferase, and we counted molts in >20 animals grown on vehicle or auxin condition. Previously, it was reported that although mutants seam cells fuse in the L3 stage and alae formation occurs precociously in *hbl-1* hypomorph animals, they execute a fourth molt (Abrahante et al., 2003). By contrast, we observed that 85% of the worms exhibited only 3 molts, and the remaining 15% showed only two molts (Figure 2.2B-C). Our result shows that more extensive HBL-1 depletion by AID system cause a fully penetrant precocious exit from the molting cycle, and suggests that this tool will allow us to better study the postembryonic role of HBL-1 in the regulation of epidermal cell fates.
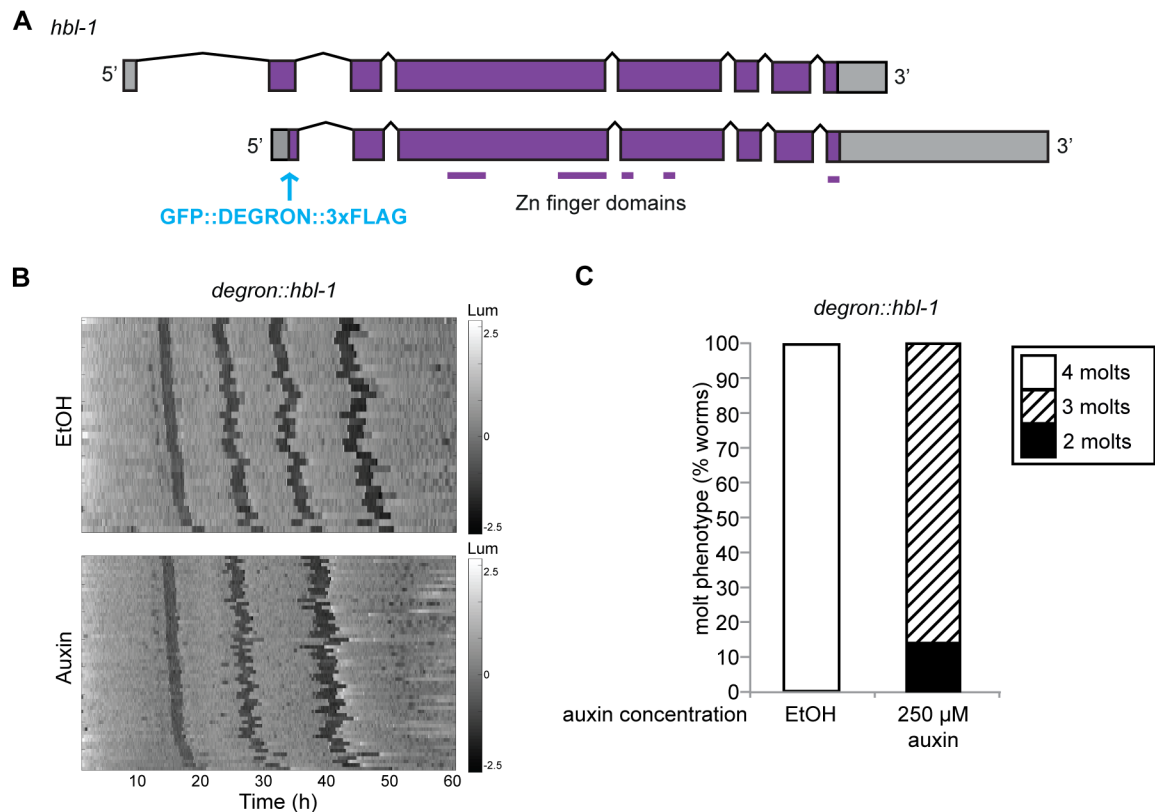
Figure 2.2 HBL-1 depletion with the AID system causes a precocious molting phenotype

(A) Schematic representation of the *hbl-1* genomic regions. Insertion of *gfp::degron::3xflag*-encoding sequence at the 5' end specifically tags HBL-1.

(B) Trend corrected heatmap showing luminescence of *degron::hbl-1* animals expressing TIR1 and luciferase from the *eft-3* promoter grown on vehicle (0.25% ethanol) or auxin (250 μM) in a temperature-controlled incubator set to 20 °C. Each line represents one animal. Hatch is set to t = 0 hours and traces are sorted by entry into the first molt. Darker color corresponds to low luminescence and is associated with the molt.

(C) Quantification of the number of molts for vehicle-treated animals (0.25% ethanol) or auxin-treated animals (250 μM auxin) (n > 20).

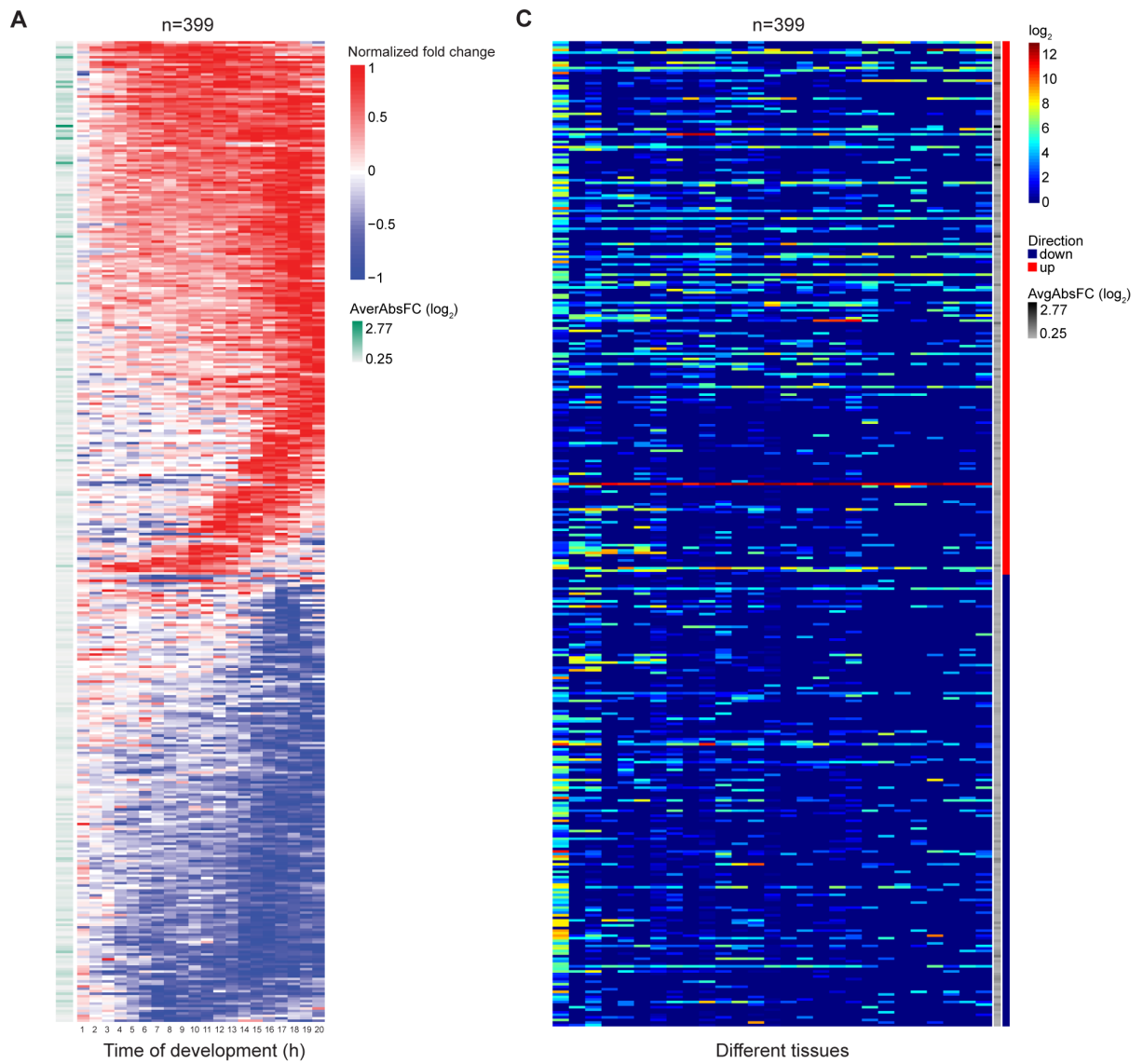### 2.2.3 HBL-1 depletion cause dysregulation of 399 genes

To gain insight into the molecular functions of HBL-1, we investigated gene expression changes upon HBL-1 depletion. To this end, we cultured a population of synchronized animals in liquid medium at 20°C. Since *hbl-1* is expressed in early stages of development, we added auxin at the beginning of the experiment (time point 0). We sampled animals hourly from 0 hours until 20 hours and performed mRNA sequencing. We identified 399 genes that differed significantly in their expression over time between vehicle and auxin conditions (Figure 2.3A). These included genes that were upregulated and genes that were downregulated in auxin-treated relative to vehicle-treated animals (Figure 2.3A). Genes were upregulated and downregulated at different times of development. The ones that are upregulated the earliest, presumably direct targets, are represented at the top of the heat map, instead the ones that are downregulated the earliest are at the bottom of the heat map (Figure 2.3A).

To further understand the functional relevance of HBL-1, we sought to examine in which tissues the genes affected by HBL-1 depletion are expressed, using a recently published tissue annotation (Cao et al., 2017). We found that the differentially expressed genes are genes expressed in the tissues in which HBL-1 is highly accumulated, meaning epidermis, neurons and intestine (Figure 2.3B). In particular, we found that genes that are changing the earliest in our dataset, are genes expressed in the intestine, whereas genes that are specifically in the epidermis are changing later in time (Figure 2.3C). This result suggests that *hbl-1* might have first an important role in the intestine regulation, and later in the epidermis. However, we have to consider that the intestinal transcriptome might be changing the earliest because more sensitive to auxin addition, so the effect that we observe in this specific tissue it might not be due to temporal activity of *hbl-1*.

2.2.3 HBL-1 depletion cause upregulation of some heterochronic genes

Among the genes that are upregulated in multiple detected tissues we identified several heterochronic genes, such as *lin-29, mab-10, lin-46, let-7* and *hbl-1* itself (Figure 2.4A). We showed previously that *hbl-1* presumably regulates only one of the two *lin-29* isoforms, i.e. *lin-29b.* However, we could not distinguish the two *lin-29* isoforms in our dataset. To validate the functional significance of this regulation by HBL-1 on *lin-29b*, we crossed the *degron::hbl-1* animals with *lin-29a(Δ)* and *lin-29b(Δ)* mutant worms. We performed luciferase assay with these animals and we observed that *lin-29b* mutation suppressed the precocious molting

phenotype with high penetrance, with 95% of the worms exiting the molting cycle after four molts (Figure 2.4B). This result is a further indication that *hbl-1* is responsible for the specific upregulation of *lin-29b*. A small percentage of the worms carrying the *lin-29a* null allele show 4 molts as well, consistent with the fact that the two *lin-29* isoforms have a redundant role in the cessation of the molting (Figure 2.4B).

A n=399

Normalized fold change
1
0.5
0
−0.5
−1

AverAbsFC (log$_2$)
2.77
0.25

Time of development (h)
1 2 3 4 5 6 7 8 9 10 11 12 13 14 15 16 17 18 19 20

C n=399

log$_2$
12
10
8
6
4
2
0

Direction
down
up

AvgAbsFC (log$_2$)
2.77
0.25

Different tissues

B

log$_2$
12
10
8
6
4
2
0

Direction
down
up

AvgAbsFC (log$_2$)
2.77
0.25

AllTissues
Epidermis
Intestine

hbl−1
7.62
0

Cholinergic neurons
GABAergic neurons
Pharyngeal neurons
Canal associated neurons
Oxygen sensory neurons
flp.1 interneurons
Touch receptor neurons
Other interneurons
Vulval precursors
Somatic gonad precursors
Sex myoblasts
Pharyngeal gland
Distal tip cells
Germline
Pharyngeal epithelia
Pharyngeal muscle
Ciliated sensory neurons
Body wall muscle
Intestinal rectal muscle
Coelomocytes
Seam cells
Socket cells
Am.PH sheath cells
Excretory cells
Non seam hypodermis
Rectum
Intestine

81

Figure 2.3 Degradation of HBL-1 affects the expression of genes in epidermis, neurons and intestine

(A) Heatmap of normalized fold change between gene expression in 250 µM auxin and in vehicle 0.25% ethanol conditions. To align the vehicle condition to the auxin condition, the gene expression over time of the vehicle condition were spline interpolated. The interpolated time points of the 1000 most changing genes in the vehicle condition that correlated best with the time points of the auxin condition were chosen as aligned 'new' time points. A generalized additive model was used to identify significant differential expression of genes between the two conditions (n=399). The normalized fold change of the two condition is clustered with 1D t-SNE map. The size effect of the changing genes is depicted in green (average absolute fold change in $\log_2$).

(B) Heatmap showing the spatial expression of genes significantly altered upon HBL-1 depletion (from (A). Every column corresponds to one gene, rows correspond to indicated tissues with tissue annotation and expression levels from L2 larvae according to (Cao et al., 2017). Genes expressed in most tissues, epidermis, or intestine are shown in violet, green, and yellow respectively. Expression of *hbl-1* in the indicated tissues is reported in pink. Red and blue bars indicate the upregulated and downregulated genes respectively. The size effect of the changing genes is depicted in grey (average absolute fold change in $\log_2$).

(C) Heatmap showing the expression of HBL-1 targets genes in cells assigned to indicated tissue (intestine, epidermis, all tissues) in Figure 2.3B, sorted according to Figure 2.3A. Red and blue bars indicate the upregulated and downregulated genes respectively. The size effect of the changing genes is depicted in grey (average absolute fold change in $\log_2$).
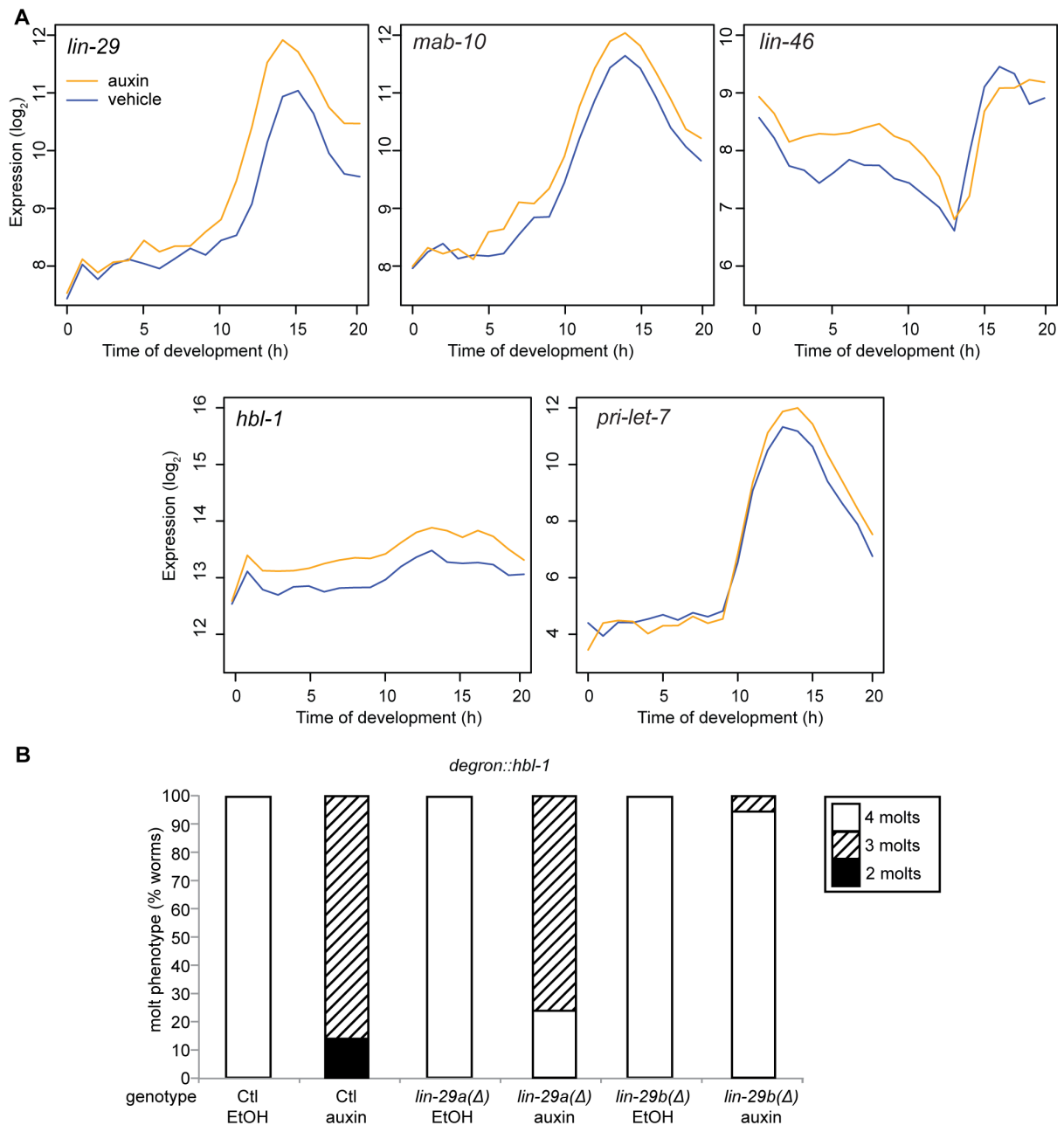
Figure 2.4 HBL-1 depletion results in upregulation of heterochronic genes

(A) Expression changes of indicated genes (*lin-29, mab-10, lin-4, hbl-1 and let-7*) in vehicle (blue) and auxin treated (orange) animals, obtained from time course in Figure 2.3.

(B) Quantification of the number of molts for vehicle-treated animals (0.25% ethanol) or auxin-treated animals (250 µM auxin) in animals expressing *gfp::degron::3xflag::hbl-1* in wild type background (Ctl) and *lin-29a(Δ)* and *lin-29b(Δ)* mutant background (n > 20).

3 Discussion

Proper development of tissues, organs and entire organisms relies on timing and coordination of cell fates. Research on heterochronic genes in *Caenorhabditis elegans* has shed light on the process by which cells in an organism keep track of developmental time. In this thesis, I propose the *C. elegans* heterochronic pathway as a powerful model to study temporal control and provide insight into mechanistic understanding of timing in animals. Furthermore, we advanced the knowledge of genetic and molecular interactions of the *C. elegans* heterochronic genes. Here, I will discuss these findings.

3.1 A branched heterochronic pathway regulates the juvenile-to-adult transition in *C. elegans*

The *C. elegans* heterochronic pathway is one of the best-characterized developmental timing pathways. However, in the literature different models of the pathway are drawn, because of the complexity of genetic interactions and the lack of knowledge of direct molecular connections among the heterochronic genes. Typically, the heterochronic pathway is depicted as a linear chain of events that trigger the J/A transition: *let-7* silences LIN-41, and relieves *lin-29* from repression by LIN-41 (Ambros, 2011; Faunes and Larraín, 2016; Rougvie and Moss, 2013). With this work, we revised this linear model, showing that the J/A transition events relies on two separate arms of the heterochronic pathway. *lin-29* occurs in two isoforms and our results demonstrate that they have partially distinct functions. This functional specificity does not come from differences in protein sequence but depends on temporally and spatially distinct expression patterns of the isoforms. Unique expression patterns are the result of isoform-specific regulation by distinct heterochronic input. Thus, the heterochronic pathway bifurcates into one arm involving *hbl-1* and *lin-29b*, and another, parallel arm that involves *lin-41*, *lin-29a*, and *mab-10*. Whereas regulation of *lin-29a* and *mab-10* through LIN-41 has been established to be direct (Aeschimann et al., 2017), it remains to be determined how HBL-1 regulates *lin-29b*. The coordination of the two branches of the heterochronic pathway is ensured by an early phase heterochronic player, namely the RNA-binding protein LIN-28. We showed that *lin-28* is upstream the pathway's branching point, consistent with its dual function of inhibitor of *let-7* biogenesis (Lehrbach et al., 2009; Van Wynsberghe et al., 2011) and positive regulator of *hbl-1* (Vadla et al., 2012).

This architecture of the pathway poses interesting questions on how time is controlled, as both isoforms are required for the completion of larval development, but each isoform

controls for specific processes to happen at specific relative times within the last larval stage of *C.elegans* development. The branching of the pathway allows for the fine tuning of the expression patterns of the isoforms in the two cell compartments of the epidermis, seam cells and hyp7, while ensuring that the highest expression of the genes is reached at the end of the L4 stage in both cell compartments. This suggests that the final levels of the direct regulator of the J/A transition will be reached at the right time, but the upstream regulators ensure that these levels are reached in different compartments at different times. In this way, the relative times at which different events are triggered could be modulated. We could ask why this particular architecture of the pathway is beneficial for the animal, since the involvement of different isoforms to specific events of the transition might reduce the robustness of the process. This is because the events of the J/A transition can be uncoupled, and then more easily perturbed. On the one hand, we could think that additional layers of regulation, that still have to be investigated, could ensure a robust coordinated execution of the J/A transition. On the other, this architecture itself could have an advantage we are not aware of and we would like to understand.

The incomplete redundancy of functions that we propose define a hierarchy of phenotype, where the molting cycle seems the most critical process for survival of the animals. In fact, it has been observed that the redundant function of both isoforms controls the end of the molting cycle. We can speculate that this redundancy ensures that even if one branch that regulates the epidermal J/A transition fails or is impaired, development is completed. Under this perspective, the worm can reach adulthood and yield progeny, even with an incomplete epidermal terminal differentiation.

3.2 A conserved pathway regulates the onset of puberty in mammals

Given the extensive conservation of the heterochronic pathway it would be curious to learn whether the architecture we identified in this work is conserved in other species. We know that the orthologues of the *C. elegans* heterochronic gene LIN-28 have been associated with the control of puberty. Specifically, LIN28B has been associated with timing of human puberty in several studies (Ong et al., 2009; Perry et al., 2009; Sulem et al., 2009), and it has been shown that LIN28A modulates the onset of puberty in mice (Zhu et al., 2010). It has been also shown that LIN28's function in controlling J/A transition in both mammals and worms occurs through *let-7* miRNA, another highly conserved heterochronic gene (Corre et al., 2016;

Van Wynsberghe et al., 2011; Zhu et al., 2010). Moreover, *let-7* mediates the *C. elegans* J/A transition through the silencing of LIN-41, orthologous to mammalian TRIM71 (Aeschimann et al., 2019), suggesting that TRIM71 might be involved in the same process in mammals. These pieces of evidence suggest that the juvenile-to-adult transition is regulated by a conserved timing mechanism from worms to humans (Faunes and Larraín, 2016; Moss and Romer-Seibert, 2014). Furthermore, heterochronic genes are known to have a relevant conserved function in timing of cell fate decisions in animal stem or progenitor cells as described in section 1.4. These functions are reported to be involved in human carcinogenesis, with *let-7* functioning as a tumor suppressor, LIN28 and TRIM71 as putative oncogenes. For these reasons, a detailed understanding of the architecture, properties and mechanisms underlying this conserved timer in *C. elegans* will expand our knowledge of time-keeping mechanisms in other systems for biological and biomedical interest.

3.3 *hbl-1* behaves as a core player of the heterochronic pathway

Our model places HBL-1 as a central, but uncharacterized, regulator of the parallel arm of the heterochronic pathway that controls *lin-29b*. The knowledge about this heterochronic gene is fragmented because the essential role of HBL-1 for embryonic viability did not permit the placement of this player in the pathway and the dissection of its function. Here, we overcome these limitations and we show that HBL-1 has the properties of a core gene of the heterochronic pathway in the regulation of the J/A transition. First, the revised model of the heterochronic pathway that we propose explains previously observed redundancies between *lin-41* and *hbl-1* (Abrahante et al., 2003). The reported enhanced precocious J/A transition at the L3-to-L4 molt of the *lin-41; hbl-1* double mutant is now explained by isoform specific regulation. On the one hand, depletion of *lin-41* causes precious upregulation of LIN-29a in the hyp7 nuclei, and on the other, deletion of *hbl-1* causes precocious upregulation of LIN-29b in the seam cell nuclei.

Secondly, our model explains the proposed dual function of HBL-1 in the regulation of seam cells fates. Specifically, from the observation of seam cell over-proliferation in *hbl-1* mutant adults, it was inferred that HBL-1 suppresses not only the adult cell fates in larvae, preventing LIN-29 precious accumulation, but also the larval cell fates in adults (Abrahante et al., 2003; Lin et al., 2003). We now demonstrate that this phenotype is the consequence of a partial precocious J/A transition at the L3 stage. In fact, the upregulation of LIN-29b in HBL-1

depleted animals cause precocious seam cell fusion. However, seam cells do not exit the cell cycle and after dividing again in the L4 stage remain trapped in the already fused seam syncytium.

Finally, we are the first to report a precocious exit from the molting cycle phenotype, enabled by temporal manipulation of HBL-1 levels using the AID system. This observation indicates that *hbl-1* plays a key role in the regulation of the epidermal J/A transition events. Early upregulation of LIN-29 causes not only a precocious fusion and alae secretion, as previously reported (Abrahante et al., 2003; Lin et al., 2003), but also a penetrant exit from the molting cycle only after three molts, sometimes even after two. To further understand the functional post-embryonic role of *hbl-1* it would be interesting to use the AID system to revisit precocious phenotype of seam cell fusion and alae secretion.

3.4 The functional role of *hbl-1* in the regulation of cell temporal identity

Hunchback plays an important role in patterning of the *Drosophila* central nervous system, where it regulates temporal specification of cell fate (Isshiki et al., 2001). Neural progenitors divide in a stem-cell like pattern, giving rise to distinct neural types, depending on the position and timing of divisions. The neural progenitors sequentially express a set of transcription factors, and the temporal identity of the differentiated cells depends on the transcription factors that are expressed at their birth (Moss and Romer-Seibert, 2014). *Hb* is the first transcription factor expressed, and asymmetric cell division gives rise to differentiated cells that maintain *hb* expression and adopt first-born temporal identity. In *hb* mutant animals, the first-born identity is skipped, and the second born fate is executed prematurely in the progeny cells. In mammals, Ikaros proteins are related to *Hunchback.* Ikaros is important in neural development promoting early fates in the cortex and in the retina. When expressed at inappropriate times, namely later in the differentiation of neural progenitors, it can generate early neurons (Elliott et al., 2008).

These phenotypes are reminiscent of those reported for *hbl-1* hypomorph allele and of the one we observed in HBL-1 AID-depleted animals. Specifically, *hbl-1* loss causes precious seam cells fusion and alae formation (Abrahante et al., 2003; Lin et al., 2003), HBL-1 depleted worms show only 3 molts. The execution of the adult seam cell fate one stage too early in *C. elegans* suggest that the role of *hunckback* proteins in programming temporal identity could have been conserved in evolution.

Moreover, ours and others' work showed that *hbl-1* is expressed in different types of neurons (Fay et al., 1999; Lin et al., 2003), suggesting that *hunchback* proteins have conserved roles in the temporal regulation of these cell types. In the literature, it is already reported that *hbl-1* acts cell autonomously to pattern synaptic remodeling of DD motoneurons, determining when remodeling is completed (Thompson-Peer et al., 2012). We are confident that further studies on *hbl-1* would uncover a role for this heterochronic gene in the different neuron types in which is expressed.

3.5 The updated expression pattern of *hbl-1* confirms its central role in the regulation of the L2-to-L3 transition

Our results, using the endogenously tagged *hbl-1* lines, show an epidermal expression pattern in contrast with previous studies, which reported that by the L1 stage, HBL-1 was no longer expressed in the seam cells, and by L2 in the hyp7 (Abbott et al., 2005; Abrahante et al., 2003). Our observation of L2 expression in seam cells could help to explain the role of *hbl-1* in the regulation of the L2-to-L3 transition proposed previously (Abbott et al., 2005). Specifically, the previously reported repression of *hbl-1* by the *let-7* sisters miRNAs in the hyp7 during the L2 stage (Abbott et al., 2005) is supported by our observation of HBL-1 downregulation by the L3 stage in this cell compartment. Recently, it has been reported that LIN-46 helps regulating the progression from L2 to L3 cell fates through repression of HBL-1. LIN-46 sequesters HBL-1 in the cytoplasm after LIN-46 itself has been released from posttranscriptional repression by LIN-28 (Ilbay and Ambros, 2019; Ilbay et al., 2019). Moreover, in these studies it was speculated that the repression of HBL-1 activity by LIN-46 functions semi-redundantly with the translational repression of HBL-1 by the *let-7* sisters miRNAs. Given the expression pattern we observed, I speculate that *let-7* sisters miRNAs are also involved in the regulation of *hbl-1* in the seam cells. Testing this hypothesis, specifically assaying HBL-1 accumulation in the seam cells in *mir-48*, *mir-84*, and *mir-241* triple mutant animals, could allow us to better understand the tissue-specific regulation of *hbl-1* in the epidermis.

3.6 *hbl-1* expression pattern does not support direct regulation of *lin-29b*

The updated protein spatial and temporal expression pattern does not explain the regulation of *lin-29b* by HBL-1. In fact, our results show that in the seam cells, *hbl-1* is

downregulated early in development, i.e. during the L2 stage, and during the L3 stage its accumulation is only detectable at low levels in the hyp7. LIN-29b, instead, begins to accumulate in the seam cells during the mid L3 stage. If we hypothesize direct regulation of *lin-29b* by HBL-1 we would expect an overlapping spatial and temporal expression of the two heterochronic genes. However, we observe a time gap between *hbl-1* downregulation and *lin-29b* expression. Assuming that we can detect functional levels of *hbl-1* protein with confocal microscopy, we hypothesize an indirect regulation of LIN-29b by HBL-1. Specifically, this indirect regulation could happen non-cell autonomously, for example by a *hbl-1*-regulated signal from hyp7 that may regulate the temporal behaviour of seam cells. We know that in *C. elegans*, hyp7 can have cell non-autonomous function as it has been shown for the specification of the fates of vulval precursor cells (VPCs). In particular, a signal from hyp7 to the neighboring VPCs inhibits an intrinsic vulval program in the precursor cells (Hedgecock and Herman, 1995; Herman and Hedgecockt, 1990). Similarly, the expression of *hbl-1* in hyp7 could inhibit *lin-29b* expression in seam cells in early stages of development. To provide functional analysis of a cell autonomous versus non-autonomous function, I propose that we could take advantage of the AID system to spatially and temporally manipulate HBL-1 levels through expression of tissue specific TIR1 and a timed addition of auxin. Using lines expressing TIR1 either in the seam cell (using *bro-1*CNE promoter) or in the hyp7 (using the *elt-3* promoter) we would be able to deplete HBL-1 only in one specific cell compartment. Hence, we could for example ask whether repression of LIN-29b in the seam cells requires HBL-1 activity in this tissue, and up to the L3 stage, after which LIN-29b starts to accumulate in wild-type animals.

Another interpretation would take into account the essential role of some unknown HBL-1 regulated factors that mediate the regulation of *lin-29b* in the seam cells. To determine the involvement of additional players in the regulation of the HBL-1-LIN-29b axis, I propose to perform an RNAi screen. Since *hbl-1* hypomorph mutant restores the *let-7* lethal phenotype, we could initially focus on a set of ~200 genes previously found to genetically interact with l*et-7* (Rausch et al., 2015). We hypothesize that among those candidates there could be a factor that suppresses the *let-7* mutant phenotype, specifically upregulating *lin-29b* expression one stage earlier upon regulation of HBL-1. We would test this hypothesis using a LIN-29b::GFP tagged line and we would screen for mutations that cause precocious accumulation of LIN-29b in early larval stages, phenocopying *hbl-1* mutation.

3.7 Uncoupling of the J/A transition events

In 1989, Victor Ambros described the epidermal J/A transition as a developmental transition characterized by four different easily detectable events: seam cells exit from the cell cycle, seam cell fusion, synthesis of adult alae and exit from the molting cycle. The epidermal J/A transition events were considered tightly coupled, because all four are triggered by the accumulation of a single gene, *lin-29*. Our data challenge this idea. Specifically, we showed that HBL-1-depleted worms and *mab-10(0) lin-29a(Δ)* double mutant adults show a striking loss of coordination of J/A transition events. In HBL-1-depleted animals we observe a penetrant precocious molting cessation phenotype and others showed precocious seam cell fusion and alae formation (Abrahante et al., 2003; Lin et al., 2003). Similarly, in *mab-10(0) lin-29a(Δ)* double mutant we observed the same hallmarks of seam cell terminal differentiation. However, in both cases seam cells fail to exit the cell cycle, since additional seam cell nuclei are observed in the adult animals. These results suggest that in seam cells, cell cycle arrest is not necessary for terminal differentiation, consequently proliferation and differentiation are not mutually exclusive processes. Thus, J/A transition events can be uncoupled and for a complete terminal differentiation of seam cells, both arms of the heterochronic pathway must be tightly coordinated.

The uncoupling of the J/A transition events suggests that it would be informative looking at these different phenotypes independently in different heterochronic mutants. In the literature, the exit from the molting cycle events is not well characterized. Specifically, precocious exit from the molting cycle has been inferred from the observation of precocious alae secretion or complete absence of seam cell division. Reiterations of the molting events, instead, were observed but it is unclear how consistently this phenotype was scored. In this work we apply an automated method that scores the exit from the molting cycle event itself, without taking in consideration other events of the J/A transition. The luciferase assay previously described in this thesis could allow an accurate characterization of the molting cycle exit of the heterochronic mutants that were not part of our study and could give insight on how these genes regulate the molting cycle. For this purpose, this assay combined with the AID degron system could allow timed manipulation of gene expression of factors that have known sequential function during larval development, such as *hbl-1* or *lin-28*.

3.8 Identification of HBL-1 targets

The analysis of the transcriptomes of wild-type and HBL-1 depleted animals allow us to identify HBL-1 targets. We identified 399 hits that are either upregulated or downregulated over time, since zinc fingers transcription factors like HBL-1 can act as transcriptional activators or repressors. The 399 genes that dynamically change over time are specifically enriched in epidermis, neurons and intestine, the tissues in which we showed HBL-1 is post-embryonically detectable. The importance of *hbl-1* activity in the neurons and epidermis is supported in the literature (Abrahante et al., 2003; Fay et al., 1999; Lin et al., 2003; Thompson-Peer et al., 2012). To our surprise, the genes that change the earliest and massively are genes enriched in the intestine. This observation, together with the sustained expression in gut nuclei throughout larval development, suggests an unknown involvement of *hbl-1* in intestine regulation. Recently, it has been shown that LIN-29 regulates genes involved in fat metabolism during normal development cell non-autonomously (Abete-Luzi et al., 2020). Ours and others' results indicate that the validation of intestine specific hits may uncover an unknown function of *hbl-1* during development.

Given our interest in the regulation of epidermal cell fates by the heterochronic pathway, we looked for misexpressed heterochronic genes in our data set. We found that *lin-29* mRNA is indeed upregulated earlier upon HBL-1 depletion, and that *lin-29b* mutation suppresses the precocious exit from the molting cycle specifically. This result further supports our hypothesis of specific regulation of *lin-29b* by HBL-1. Interestingly, we found that *pri-let-7* is modestly upregulated upon HBL-1 depletion, supporting the previously shown transcriptional repression of primary *let-7* (Roush and Slack, 2009). Finally, *hbl-1* mRNA is upregulated upon HBL-1 protein degradation, suggesting that HBL-1 controls its own transcription via a negative feedback loop, which could be direct or mediated by an unknown factor. Performing a ChIP-Seq experiment using the endogenously tagged GFP::HBL-1 could complement the transcriptomics-based target identification, and could allow us to understand if *lin-29b*, *pri-let-7* and *hbl-1* regulation by HBL-1 occurs at the transcription level. Further analysis of the genes with a heterochronic function or genes with spatial and temporal expression patterns in wild-type animals consistent with regulation by *hbl-1* could help to better understand the role of *hbl-1* in regulation of epidermis development. Using RNAi, for example, we can look for factors that genetically interact with *hbl-1*, suppressing or phenocopying *hbl-1* mutant phenotypes. Relevant candidates could be further validated on

the one hand, through observation of expression of endogenously tagged genes, on the other through analysis of the effect of their mutations on the expression of other heterochronic genes, especially *lin-29b*.

In conclusion, we consider HBL-1 a critical player in the heterochronic pathway, and a better characterization of this transcription factor activity may transform our understanding of how the heterochronic pathway establishes temporal patterning, and our knowledge of molecular timekeeping mechanisms in general.

4 Methods

This chapter describes the methods used in section 2.2.

C. elegans handling

Worm strains used in this study are listed in Key resources table. Bristol N2 was used as the wild- type strain. Animals were synchronized by extraction of the embryos from gravid adults using a bleaching solution (30% (v/v) sodium hypochlorite (5% chlorine) reagent (Thermo Fisher Scientific; 419550010), 750 mM KOH) and hatching overnight in the absence of food, at room temperature in M9 buffer (42 mM Na2HPO4, 22 mM KH2PO4, 86 mM NaCl, 1 mM MgSO4). Synchronized arrested L1 larvae (L1s) were grown on 2% NGM agar plates with Escherichia coli OP50 bacteria (Stiernagle, 2006). For microscopy, animals were mounted on a 2% (w/v) agarose pad and immobilized in 10 mM levamisol (Fluca Analytical, 31742).

Generation of endogenously tagged *hbl-1* using CRISPR-Cas9

In order to specifically tag *hbl-1* at the N-terminus with *gfp* and *gfp::degron::3xflag* tag the following mix was injected in wild-type worms: 0.25 ug/ul Cas9, 0.1ug/ul tracRNA, 0.05 ug/ul crRNA (gtccaactttctaattttgt), 4ug of hybridized DNA used as donors, 20ng/ul of pIK127 (eft-3::gfp) and 40 ng/ul of pRF4(rol-6) as co-injection markers, as described in (Dokshin et al., 2018).

Confocal imaging

For confocal imaging of endogenously tagged HBL-1, worms were grown at 25˚C for 8 hr, 15 hr, 20 hr and 25 hr. Worms were imaged on an Axio Imager M2 (upright microscope) + Yokogawa CSU W1 Dual camera T2 spinning disk confocal scanning unit driven by Visiview 3.1.0.3. Differential Interference Contrast (DIC) and fluorescent images were acquired with a 40x/1.3 oil immersion objective (2048 x 2048 pixels, 16 bits). Using the Fiji software (Schindelin et al., 2012), images were processed after selecting representative regions.

Luciferase assay

Luciferase assays were performed as described (Meeuse et al., 2020). Briefly, embryos were extracted from gravid adults using a bleaching solution. Single embryos were transferred into a well of a white, flat-bottom, 384-well plate (Berthold Technologies, 32505) by pipetting.

Animals were left to develop in 90 mL S-Basal medium containing E. coli OP50 (OD600 = 0.9), 100 mM Firefly D-Luciferin (p.j.k., 102111) and either vehicle (0.25% Ethanol) or 3-indoleacetic acid (auxin, Sigma Aldrich, I2886) in 100% Ethanol (final concentration 250 uM). Plates were sealed with Breathe Easier sealing membrane (Diversified Biotech, BERM-2000). Luminescence was measured using a luminometer (Berthold Technologies, Centro XS3 LB 960) every 10 min for 0.5 s for 72 or 100 hr in a temperature-controlled incubator set to 20˚C. Luminescence data was analyzed using an automated algorithm to detect the hatch and the molts (Meeuse et al., 2020).

RNA-seq time course

Synchronized L1 worms were cultured in liquid culture (S-Basal supplemented with OP50, OD600=2.6, 1000 animals/mL) in a temperature controlled incubator at 20°C with 120 rpm. At time point zero, in the experimental worms' culture 250 µM auxin or in the control worms' culture 0.25% ethanol (vehicle), was added. We harvested hourly from 0 hours until 20 hours of development. At each time point 15.000, 10.000 or 7.500 animals, depending on the developmental stage (L1, L2 and L3 respectively), were collected and washed three additional times with M9 buffer (42 mM Na2HPO4, 22 mM KH2PO4, 86 mM NaCl, 1 mM MgSO4) for RNA extraction.

RNA extraction and sequencing library preparation

Pelleted animals were resuspended in Tri Reagent (MRC, TR118) and RNA was extracted using conventional phenol extraction, as described previously (Hendriks et al., 2014). Total RNA was DNAse treated and libraries were prepared using the TruSeq Illumina mRNA-seq (stranded – high input) protocol. Libraries were sequenced using the NextSeq HIGH-OUT 75 cycles paired-end reads protocol on the NextSeq 550.

5 Supplemental tables

This chapter reports table related to section 2.2.

Worm strains used in this study

Identifier/ Strain number	Genotype
N2	Wild-type
HW2704	*hbl-1 [(xe191) gfp::hbl-1]X*
HW2833	*xeSi376[Peft-3::TIR-1::mRuby::unc-54 3'UTR] III; hbl-1 [(xe201) gfp::Degron:: 3xFLAG::hbl-1]X*
HW3025	*xeSi376[Peft-3::TIR-1::mRuby::unc-54 3'UTR] III; xeSi312 [Peft-3::luc::gfp::unc-54 3'UTR, unc-119(+)] IV; hbl-1 [(xe201) gfp::Degron::3xFLAG::hbl-1] X*
HW3151	*lin-29(xe40)II; xeSi376[Peft-3::TIR-1::mRuby::unc-54 3'UTR] III; xeSi312 [Peft-3::luc::gfp::unc-54 3'UTR, unc-119(+)] IV; hbl-1 [(xe201) gfp-::Degron::3xFLAG::hbl-1] X*
HW3152	*lin-29(xe120)II; xeSi376[Peft-3::TIR-1::mRuby::unc-54 3'UTR] III; xeSi312 [Peft-3::luc::gfp::unc-54 3'UTR, unc-119(+)] IV; hbl-1 [(xe201) gfp-::Degron::3xFLAG::hbl-1] X*
HW3153	*lin-46(ma385) I; xeSi376[Peft-3::TIR-1::mRuby::unc-54 3'UTR] III; xeSi312 [Peft-3::luc::gfp::unc-54 3'UTR, unc-119(+)] IV; hbl-1 [(xe201) gfp-::Degron::3xFLAG::hbl-1] X*

Quantification of number of molts, raw data related to Figure 2.2B

worm line	2 molts	3 molts	4 molts	total number of worms
HW2833 EtOh	0	0	47	47
HW2833 250 uM auxin	12	88	0	96

Quantification of number of molts, raw data related to Figure 2.4B

worm line	2 molts	3 molts	4 molts	total number of worms
HW2833 EtOh	0	0	54	54
HW2833 250 uM auxin	9	52	0	61
HW3151 EtOh	0	0	55	55
HW3151 250 uM auxin	0	54	19	73
HW3152 EtOh	0	0	22	27
HW3152 250 uM auxin	0	2	27	29

6 References

Abbott, A.L. (2011). Uncovering new functions for MicroRNAs in caenorhabditis elegans. Curr. Biol. *21*, R668–R671.

Abbott, A.L., Alvarez-Saavedra, E., Miska, E.A., Lau, N.C., Bartel, D.P., Horvitz, H.R., and Ambros, V. (2005). The let-7 MicroRNA family members mir-48, mir-84, and mir-241 function together to regulate developmental timing in Caenorhabditis elegans. Dev. Cell *9*, 403–414.

Abete-Luzi, P., Fukushige, T., Yun, S., Krause, M.W., and Eisenmann, D.M. (2020). New roles for the heterochronic transcription factor lin-29 in cuticle maintenance and lipid metabolism at the larval-to-adult transition in caenorhabditis elegans. Genetics *214*, 669–690.

Abrahante, J.E., Daul, A.L., Li, M., Volk, M.L., Tennessen, J.M., Miller, E.A., and Rougvie, A.E. (2003). The Caenorhabditis elegans hunchback-like gene lin-57/hbl-1 controls developmental time and is regulated by microRNAs. Dev. Cell *4*, 625–637.

Aeschimann, F., Kumari, P., Bartake, H., Gaidatzis, D., Xu, L., Ciosk, R., and Großhans, H. (2017). LIN41 Post-transcriptionally Silences mRNAs by Two Distinct and Position-Dependent Mechanisms. Mol. Cell *65*, 476-489.e4.

Aeschimann, F., Neagu, A., Rausch, M., and Großhans, H. (2019). Let-7 coordinates the transition to adulthood through a single primary and four secondary targets. Life Sci. Alliance *2*, 1–18.

Alsiö, J.M., Tarchini, B., Cayouette, M., and Livesey, F.J. (2015). Ikaros promotes early-born neuronal fates in the cerebral cortex. Proc. Natl. Acad. Sci. U. S. A. *112*, E3088.

Ambros, V. (1989). A hierarchy of regulatory genes controls a larva-to-adult developmental switch in C. elegans. Cell *57*, 49–57.

Ambros, V. (2011). MicroRNAs and developmental timing. Curr. Opin. Genet. Dev. *21*, 511–517.

Ambros, V., and Horvitz, H.R. (1984). Heterochronic mutants of the nematode Caenorhabditis elegans. Science (80-.). *226*, 409–416.

Ambros, V., and Horvitz, R.H. (1987). The lin-14 locus of Caenorhabditis elegans controls the time of expression of specific postembryonic developmental events. Genes Dev. 398–414.

Arasu, P., and Hospital, M.G. (1991). Temporal regulation of lin-14 by the antagonistic action of two other heterochronic genes , lin-4 and lin-28. Genes Dev. 1825–1833.

Azzi, C., Aeschimann, F., Neagu, A., and Großhans, H. (2020). A branched heterochronic pathway directs juvenile-to-adult transition through two LIN-29 isoforms. Elife 1–28.

Balzer, E., Heine, C., Jiang, Q., Lee, V.M., and Moss, E.G. (2010). LIN28 alters cell fate succession and acts independently of the let-7 microRNA during neurogliogenesis in vitro. Development *137*, 891–900.

Bartel, D.P. (2009). MicroRNAs: Target Recognition and Regulatory Functions. Cell *136*, 215–233.

Bettinger, J.C., Lee, K., and Rougvie, A.E. (1996). Stage-specific accumulation of the terminal differentiation factor LIN-29 during Caenorhabditis elegans development. Development *122*, 2517–2527.

Bettinger, J.C., Euling, S., and Rougvie, A.E. (1997). The terminal differentiation factor LIN-29 is required for proper vulval morphogenesis and egg laying in Caenorhabditis elegans. Development *124*, 4333–4342.

Brancati, G., and Großhans, H. (2018). An interplay of miRNA abundance and target site architecture determines miRNA activity and specificity. Nucleic Acids Res. *46*, 3259–3269.

Cao, J., Packer, J.S., Ramani, V., Cusanovich, D.A., Huynh, C., Daza, R., Qiu, X., Lee, C., Furlan, S.N., Steemers, F.J., et al. (2017). Comprehensive single-cell transcriptional profiling of a

multicellular organism. Science (80-.). *357*, 661–667.

Cassada, R.C., and Russell, R.L. (1975). The dauerlarva, a post-embryonic developmental variant of the nematode Caenorhabditis elegans. Dev. Biol. *46*, 326–342.

Chang, H.M., Martinez, N.J., Thornton, J.E., Hagan, J.P., Nguyen, K.D., and Gregory, R.I. (2012). Trim71 cooperates with microRNAs to repress Cdkn1a expression and promote embryonic stem cell proliferation. Nat. Commun. *3*.

Chen, Y.L., Yuan, R.H., Yang, W.C., Hsu, H.C., and Jeng, Y.M. (2013). The stem cell E3-ligase Lin-41 promotes liver cancer progression through inhibition of microRNA-mediated gene silencing. J. Pathol. *229*, 486–496.

Chishom, A.D., and Hsiao, T.I. (2012). The C. elegans epidermis as a model skin. I: development, patterning, and growth. Wiley Interdiscip Rev Dev Biol. 861–878.

Corre, C., Shinoda, G., Zhu, H., Cousminer, D.L., Crossman, C., Bellissimo, C., Goldenberg, A., Daley, G.Q., and Palmert, M.R. (2016). Sex-specific regulation of weight and puberty by the Lin28/let-7 axis. J. Endocrinol. *228*, 179–191.

Corsi, A.K., Wightman, B., and Chalfie, M. (2015). A transparent window into biology: A primer on Caenorhabditis elegans. Genetics *200*, 387–407.

Cuevas, E., Rybak-Wolf, A., Rohde, A.M., Nguyen, D.T.T., and Wulczyn, F.G. (2015). Lin41/Trim71 is essential for mouse development and specifically expressed in postnatal ependymal cells of the brain. Front. Cell Dev. Biol. *3*, 1–13.

Dokshin, G.A., Ghanta, K.S., Piscopo, K.M., and Mello, C.C. (2018). Robust Genome Editing with Short Single-Stranded. Genetics *210*, 781–787.

Du, N., Kwon, H., Li, P., West, E.E., Oh, J., Liao, W., Yu, Z., Ren, M., and Leonard, W.J. (2014). EGR2 is critical for peripheral naïve T-cell differentiation and the T-cell response to influenza. Proc. Natl. Acad. Sci. U. S. A. *111*, 16484–16489.

Ecsedi, M., Rausch, M., and Großhans, H. (2015). The let-7 microRNA directs vulval development through a single target. Dev. Cell *32*, 335–344.

Elliott, J., Jolicoeur, C., Ramamurthy, V., and Cayouette, M. (2008). Ikaros Confers Early Temporal Competence to Mouse Retinal Progenitor Cells. Neuron *60*, 26–39.

Faunes, F., and Larraín, J. (2016). Conservation in the involvement of heterochronic genes and hormones during developmental transitions. Dev. Biol. *416*, 3–17.

Fay, D.S., Stanley, H.M., Han, M., and Wood, W.B. (1999). A Caenorhabditis elegans homologue of hunchback is required for late stages of development but not early embryonic patterning. Dev. Biol. *205*, 240–253.

Frøkjær-Jensen, C., Davis, M.W., Sarov, M., Taylor, J., Flibotte, S., LaBella, M., Pozniakovsky, A., Moerman, D.G., and Jorgensen, E.M. (2014). Random and targeted transgene insertion in Caenorhabditis elegans using a modified Mos1 transposon. Nat. Methods *11*, 529–534.

Großhans, H., Johnson, T., Reinert, K.L., Gerstein, M., and Slack, F.J. (2005). The temporal patterning microRNA let-7 regulates several transcription factors at the larval to adult transition in C. elegans. Dev. Cell *8*, 321–330.

Harris, D.T., and Horvitz, R.H. (2011). MAB-10/NAB acts with LIN-29/EGR to regulate terminal differentiation and the transition from larva to adult in C. elegans. Development *138*, 4051–4062.

Hedgecock, E.M., and Herman, R.K. (1995). The ncl-1 gene and genetic mosaics of Caenorhabditis elegans. Genetics *141*, 989–1006.

Hendriks, G.J., Gaidatzis, D., Aeschimann, F., and Großhans, H. (2014). Extensive Oscillatory Gene Expression during C.elegans Larval Development. Mol. Cell *53*, 380–392.

Herman, R.K., and Hedgecockt, E.M. (1990). Limitation of the size of the vulval primordium of

Caenorhabditis elegans by lin-15 expression in surrounding hypodermis. Nature *348*, 169–171.

Hubaud, A., and Pourquié, O. (2014). Signalling dynamics in vertebrate segmentation. Nat. Rev. Mol. Cell Biol. *15*, 709–721.

Hunter, S.E., Finnegan, E.F., Zisoulis, D.G., Lovci, M.T., Melnik-Martinez, K. V., Yeo, G.W., and Pasquinelli, A.E. (2013). Functional Genomic Analysis of the let-7 Regulatory Network in Caenorhabditis elegans. PLoS Genet. *9*.

Ilbay, O., and Ambros, V. (2019). Regulation of nuclear-cytoplasmic partitioning by the lin-28-lin-46 pathway reinforces microRNA repression of HBL-1 to confer robust cell-fate progression in C. Elegans. Dev. *146*.

Ilbay, O., Nelson, C., and Ambros, V. (2019). C.elegans LIN-28 controls temporal cell-fate progression by regulating LIN-46 expression via the 5'UTR of lin-46 mRNA. BioRxiv 697490.

Isshiki, T., Pearson, B., Holbrook, S., and Doe, C.Q. (2001). Drosophila neuroblasts sequentially express transcription factors which specify the temporal identity of their neuronal progeny. Cell *106*, 511–521.

John, L.B., and Ward, A.C. (2011). The Ikaros gene family: Transcriptional regulators of hematopoiesis and immunity. Mol. Immunol. *48*, 1272–1278.

Keyte, A.L., and Smith, K.K. (2015). Ontogenies in Evolution. Semin Cell Dev Biol 99–107.

Kimble, J., and Hirsh, D. (1979). The postembrionic cell lineage of the Hermaphrodite and male gonads in Caenorhabditis elegans. Dev Biol *70*, 396–417.

Kmita, M., and Duboule, D. (2003). Organizing axes in time and space; 25 years of colinear tinkering. Science (80-.). *301*, 331–333.

Kohwi, M., and Doe, C.Q. (2013). Temporal fate specification and neural progenitor competence during development. Nat. Rev. Neurosci. *14*, 823–838.

Laslo, P., Spooner, C.J., Warmflash, A., Lancki, D.W., Lee, H.J., Sciammas, R., Gantner, B.N., Dinner, A.R., and Singh, H. (2006). Multilineage Transcriptional Priming and Determination of Alternate Hematopoietic Cell Fates. Cell *126*, 755–766.

Le, N., Nagarajan, R., Wang, J.Y.T., Svaren, J., LaPash, C., Araki, T., Schmidt, R.E., and Milbrandt, J. (2005). Nab proteins are essential for peripheral nervous system myelination. Nat. Neurosci. *8*, 932–940.

Lee, R.C., Feinbaum, R.L., and Ambros, V. (1993). The C . elegans Heterochronic Gene lin-4 Encodes Small RNAs with Antisense Complementarity to lin-14. Cell *75*, 843–854.

Lehrbach, N.J., Armisen, J., Lightfoot, H.L., Murfitt, K.J., Bugaut, A., Balasubramanian, S., and Miska, E.A. (2009). LIN-28 and the poly(U) polymerase PUP-2 regulate let-7 microRNA processing in Caenorhabditis elegans. Nat. Struct. Mol. Biol. *16*, 1016–1020.

Lin, S.Y., Johnson, S.M., Abraham, M., Vella, M.C., Pasquinelli, A., Gamberi, C., Gottlieb, E., and Slack, F.J. (2003). The C. elegans hunchback homolog, hbl-1, controls temporal patterning and is a probable MicroRNA target. Dev. Cell *4*, 639–650.

Loedige, I., Gaidatzis, D., Sack, R., Meister, G., and Filipowicz, W. (2013). The mammalian TRIM-NHL protein TRIM71/LIN-41 is a repressor of mRNA function. Nucleic Acids Res. *41*, 518–532.

Meeuse, M.W., Hauser, Y.P., Morales Moya, L.J., Hendriks, G., Eglinger, J., Bogaarts, G., Tsiairis, C., and Großhans, H. (2020). Developmental function and state transitions of a gene expression oscillator in Caenorhabditis elegans . Mol. Syst. Biol. *16*, 1–21.

Min, I.M., Pietramaggiori, G., Kim, F.S., Passegué, E., Stevenson, K.E., and Wagers, A.J. (2008). The Transcription Factor EGR1 Controls Both the Proliferation and Localization of Hematopoietic Stem Cells. Cell Stem Cell *2*, 380–391.

Moss, E.G. (2007). Heterochronic Genes and the Nature of Developmental Time. Curr. Biol. *17*, 425–434.

Moss, E.G., and Romer-Seibert, J. (2014). Cell-intrinsic timing in animal development. Wiley Interdiscip. Rev. Dev. Biol. *3*, 365–377.

Moss, E.G., and Tang, L. (2003). Conservation of the heterochronic regulator Lin-28, its developmental expression and microRNA complementary sites. Dev. Biol. *258*, 432–442.

Moss, E.G., Lee, R.C., and Ambros, V. (1997). The cold shock domain protein LIN-28 controls developmental timing in C. elegans and is regulated by the lin-4 RNA. Cell *88*, 637–646.

Nguyen, H.Q., Hoffman-Liebermann, B., and Liebermann, D.A. (1993). The zinc finger transcription factor Egr-1 is essential for and restricts differentiation along the macrophage lineage. Cell *72*, 197–209.

Olmedo, M., Geibel, M., Artal-Sanz, M., and Merrow, M. (2015). A high-throughput method for the analysis of larval developmental phenotypes in Caenorhabditis elegans. Genetics *201*, 443–448.

Ong, K.K., Elks, C.E., Li, S., Zhao, J.H., Luan, J., Andersen, L.B., Bingham, S.A., Brage, S., Smith, G.D., Ekelund, U., et al. (2009). Genetic variation in LIN28B is associated with the timing of puberty. Nat. Genet. *41*, 729–733.

Perry, J.R.B., Stolk, L., Franceschini, N., Lunetta, K.L., Zhai, G., McArdle, P.F., Smith, A. V., Aspelund, T., Bandinelli, S., Boerwinkle, E., et al. (2009). Meta-analysis of genome-wide association data identifies two loci influencing age at menarche. Nat. Genet. *41*, 648–650.

Rausch, M., Ecsedi, M., Bartake, H., Müllner, A., and Großhans, H. (2015). A genetic interactome of the let-7 microRNA in C. elegans. Dev. Biol. *401*, 276–286.

Reinhart, B.J., Slack, F.J., Basson, M., Pasquienelll, A.E., Bettlnger, J.C., Rougvle, A.E., Horvitz, H.R., and Ruvkun, G. (2000). The 21-nucleotide let-7 RNA regulates developmental timing in Caenorhabditis elegans. Nature *403*, 901–906.

Del Rio-Albrechtsen, T. Del, Kiontke, K., Chiou, S., and Fitch, D.H.A. (2006). Novel gain-of-function alleles demonstrate a role for the heterochronic gene lin-41 in C . elegans male tail tip morphogenesis. Dev. Biol. *297*, 74–86.

Rougvie, A.E. (2001). Control of developmental timing in animals. Nat. Rev. Genet. *2*, 690–701.

Rougvie, A.E., and Ambros, V. (1995). The heterochronic gene lin-29 encodes a zinc finger protein that controls a terminal differentiation event in Caenorhabditis elegans. Development *121*, 2491–2500.

Rougvie, A.E., and Moss, E.G. (2013). Developmental transitions in C. elegans larval stages. Curr. Top. Dev. Biol. *105*, 153–180.

Roush, S., and Slack, F.J. (2008). The let-7 family of microRNAs. Cell 505–516.

Roush, S.F., and Slack, F.J. (2009). Transcription of the C. elegans let-7 microRNA is temporally regulated by one of its targets, hbl-1. Dev. Biol. *334*, 523–534.

Ruvkun, G., and Giusto, J. (1989). The Caenorhabditis elegans heterochronic gene lin-14 encodes a nuclear protein that forms a temporal developmental switch. Nature *338*, 313–319.

Rybak, A., Fuchs, H., Smirnova, L., Brandt, C., Pohl, E.E., Nitsch, R., and Wulczyn, F.G. (2008). A feedback loop comprising lin-28 and let-7 controls pre-let-7 maturation during neural stem-cell commitment. Nat. Cell Biol. *10*, 987–993.

Schindelin, J., Arganda-Carreras, I., Frise, E., Kaynig, V., Longair, M., Pietzsch, T., Preibisch, S., Rueden, C., Saalfeld, S., Schmid, B., et al. (2012). Fiji: An open-source platform for biological-image analysis. Nat. Methods *9*, 676–682.

Shyh-Chang, N., and Daley, G.Q. (2013). Lin28: Primal regulator of growth and metabolism in stem cells. Cell Stem Cell *12*, 395–406.

Singh, J.E., and Sulston, R.N. (1978). Some observation on moulting in Caenorhabditis elegans. Nematologica 63–71.

Slack, F.J., Basson, M., Liu, Z., Ambros, V., Horvitz, H.R., and Ruvkun, G. (2000). The lin-41 RBCC gene acts in the C. elegans heterochronic pathway between the let-7 regulatory RNA and the LIN-29 transcription factor. Mol. Cell *5*, 659–669.

Smith, K.K. (2002). Sequence heterochrony and the evolution of development. J. Morphol. *252*, 82–97.

Smith, K.K. (2003). Time's arrow: Heterochrony and the evolution of development. Int. J. Dev. Biol. *47*, 613–621.

Stiernagle, T. (2006). Maintenance of C.elegans. WormBook, Ed. C. Elegans Res. Community, Wormb.

Sulem, P., Gudbjartsson, D.F., Rafnar, T., Holm, H., Olafsdottir, E.J., Olafsdottir, G.H., Jonsson, T., Alexandersen, P., Feenstra, B., Boyd, H.A., et al. (2009). Genome-wide association study identifies sequence variants on 6q21 associated with age at menarche. Nat. Genet. *41*, 734–738.

Sulston, J.E., and Horvitz, H.R. (1977). Post-embryonic cell lineages of the nematode, *Caenorhabditis elegans*. Dev Biol *56*, 110–156.

Thompson-Peer, K.L., Bai, J., Hu, Z., and Kaplan, J.M. (2012). HBL-1 Patterns Synaptic Remodeling in C . elegans. Neuron *73*, 453–465.

Thummel, C.S. (2001). Molecular Mechanisms of Developmental Timing in C. elegans and Drosophila. Dev. Cell *1*, 453–465.

Toma, K., Wang, T.C., and Hanashima, C. (2016). Encoding and decoding time in neural development. Dev. Growth Differ. *58*, 59–72.

Topilko, P., Schneider-Maunoury, S., Levi, G., Baron-Van Evercooren, A., Chennoufi, A.B.Y., Seitanidou, T., Babinet, C., and Charnay, P. (1994). Krox-20 controls myelination in the peripheral nervous system. Nature *371*, 796–799.

Vadla, B., Kemper, K., Alaimo, J., Heine, C., and Moss, E.G. (2012). Lin-28 controls the succession of cell fate choices via two distinct activities. PLoS Genet. *8*.

Vella, M.C., Choi, E., Lin, S., Reinert, K., and Slack, F.J. (2004). The C . elegans microRNA let-7 binds to imperfect let-7 complementary sites from the lin-41 3'UTR. Genes Dev. 132–137.

Viswanathan, S.R., Daley, G.Q., and Gregory, R.I. (2008). Selective Blockade of MicroRNA Processing by Lin28. Science (80-.). *320*, 97–101.

Welte, T., Tuck, A.C., Papasaikas, P., Carl, S.H., Flemr, M., Knuckles, P., Rankova, A., Bühler, M., and Großhans, H. (2019). The RNA hairpin binder TRIM71 modulates alternative splicing by repressing MBNL1. Genes Dev. *33*, 1221–1235.

Wightman, B., Ha, I., and Ruvkun, G. (1993). Posttranscriptional Regulation of the Heterochronic Gene lin-14 by W -4 Mediates Temporal Pattern Formation in C . elegans. Cell *75*, 855–862.

Worringer, K.A., Rand, T.A., Hayashi, Y., Sami, S., Takahashi, K., Tanabe, K., Narita, M., Srivastava, D., and Yamanaka, S. (2014). The let-7/LIN-41 pathway regulates reprogramming to human induced pluripotent stem cells by controlling expression of prodifferentiation genes. Cell Stem Cell *14*, 40–52.

Van Wynsberghe, P.M., Kai, Z.S., Massirer, K.B., Burton, V.H., Yeo, G.W., and Pasquinelli, A.E. (2011). LIN-28 co-transcriptionally binds primary let-7 to regulate miRNA maturation in Caenorhabditis elegans. Nat. Struct. Mol. Biol. *18*, 302–308.

Yang, D.H., and Moss, E.G. (2003). Temporally regulated expression of Lin-28 in diverse tissues of the developing mouse. Gene Expr. Patterns *3*, 719–726.

Ye, J., and Blelloch, R. (2014). Regulation of pluripotency by RNA binding proteins. Cell Stem Cell *15*, 271–280.

Yu, J., Vodyanik, M.A., Smuga-Otto, K., Antosiewicz-Bourget, J., Frane, J.L., Tian, S., Nie, J., Jonsdottir, G.A., Ruotti, V., Stewart, R., et al. (2007). Induced pluripotent stem cell lines derived from human somatic cells. Science (80-.). *318*, 1917–1920.

Zhang, L., Ward, J.D., Cheng, Z., and Dernburg, A.F. (2015). The auxin-inducible degradation (AID) system enables versatile conditional protein depletion in C. elegans. Dev. *142*, 4374–4384.

Zhu, H., Shah, S., Shyh-Chang, N., Shinoda, G., Einhorn, W.S., Viswanathan, S.R., Takeuchi, A., Grasemann, C., Rinn, J.L., Lopez, M.F., et al. (2010). Lin28a transgenic mice manifest size and puberty phenotypes identified in human genetic association studies. Nat. Genet. *42*, 626–630.

7 Acknowledgments

A special thank you to Marco, I was your chaperone once, but you have been my chaperone for the past three years. Thank you for teaching me how to be an Illustrator, for solving all my stupid problems with the pc and to listen to me whenever I wanted to talk for hours.

I want to thank all my friends, the ones here in Basel and the ones spread around the globe. Each of you made my life funnier, easier, better. I am so grateful you all supported me in this crazy journey, but our adventures are not over. You will be stuck with me for looooong time. Silvia, grazie, senza di te non ce l'avrei mai fatta e ricorda 'Eclissi del cuore saràààààààà'.

Grazie Andrea, per aver condiviso questo viaggio insieme dal primo giorno. E infine grazie a mamma, papà e Giulia per avermi sopportato e supportato in questi anni lontano da casa. Vi voglio bene!